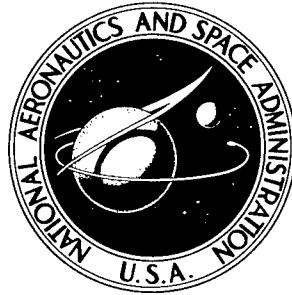


033490

<sup>1</sup>  
NASA TECHNICAL NOTE



<sup>5</sup>  
NASA TN D-3248

NASA TN D-3248

AMPTIAC

DISTRIBUTION STATEMENT A  
Approved for Public Release  
Distribution Unlimited

# MECHANICAL PROPERTIES OF SOLID-SOLUTION AND CARBIDE-STRENGTHENED ARC-MELTED TUNGSTEN ALLOYS

*by Peter L. Raffo and William D. Klopp*

*Lewis Research Center<sup>5</sup>  
Cleveland, Ohio*

20020320 232

NASA TN D-3248

MECHANICAL PROPERTIES OF SOLID-SOLUTION AND CARBIDE-  
STRENGTHENED ARC-MELTED TUNGSTEN ALLOYS

By Peter L. Raffo and William D. Klopp

Lewis Research Center  
Cleveland, Ohio

NATIONAL AERONAUTICS AND SPACE ADMINISTRATION

---

For sale by the Clearinghouse for Federal Scientific and Technical Information  
Springfield, Virginia 22151 - Price \$2.00

W  
 W-C  
 W-C-C  
 W-T-C  
 W-H-C  
 W-H-C  
 W-H-C  
 W-H-C  
 W-H-C  
 W-H-C  
 W-H-C  
 W-H-C

# MECHANICAL PROPERTIES OF SOLID-SOLUTION AND CARBIDE-

## STRENGTHENED ARC-MELTED TUNGSTEN ALLOYS\*

by Peter L. Raffo and William D. Klopp

Lewis Research Center

### SUMMARY

The mechanical properties of several arc-melted tungsten alloys containing rhenium, tantalum, columbium, hafnium and/or carbon were investigated in the temperature range 2500° to 4000° F. Solid-solution strengthening in tungsten alloys was most effective in tungsten-hafnium alloys and least effective in tungsten-rhenium alloys. The strengths of ternary alloys could be adequately represented as the sum of the individual strengthening effects found in the binary alloys. Carbon additions to unalloyed tungsten produce a minimum in the tensile-strength carbon-content curve. Carbon additions to tungsten-columbium, tungsten-tantalum, tungsten-tantalum-rhenium, and tungsten-hafnium alloys produced various degrees of strengthening with the largest effect found in the tungsten-hafnium-carbon alloys. The differences in strength between the various carbide-strengthened alloys were a result of the differences in the carbide particle size, where the finest particle size was observed in the tungsten-hafnium-carbon alloys. The strongest alloy, tungsten - 0.20 atom percent hafnium - 0.26 atom percent carbon, had a tensile strength of 62 500 pounds per square inch at 3500° F in the as-swaged condition, and recrystallized only after annealing for 4 hours at 4200° F.

The effectiveness of solid-solution strengthening could be correlated with the difference in atom size between the solute and tungsten, with larger differences promoting greater strengthening. Carbon additions to tungsten produced a decrease in strength, probably as a result of an increase in the self-diffusion rate of tungsten, as was noted previously by other investigators in gamma iron.

### INTRODUCTION

Tungsten appears to be one of the most important metallic materials being

\*Portions of the data in this report were presented at the AIME Technical Conference on Physical Metallurgy of Refractory Metals, French Lick, Indiana, October 3-5, 1965.

considered for structural use in aerospace applications at temperatures above 2500° F. It has been shown previously by a number of investigators that the high-temperature tensile and creep strengths of tungsten may be substantially increased by alloying (refs. 1 to 6). Both solid-solution and dispersion strengthening were found to be effective. In a previous study by the present authors (ref. 1), it was shown that (1) the tensile and creep strengths of arc-melted tungsten (W) at 2500° to 3500° F were increased in decreasing order of effectiveness by hafnium (Hf), tantalum (Ta), columbium (Cb), and rhenium (Re), and (2) additions of carbon (C) to a nominally W - 1 atom percent Cb alloy resulted in a further increase in strength over that of the W-Cb binary alloy due to stabilization of the cold-worked structure by carbide precipitates.

The present study was aimed at exploring the W-Hf system in more detail and examining the properties of several ternary alloys containing the above-mentioned alloy additions. The strengthening mechanisms associated with the various alloying elements were studied. Also, additional studies on the effects of carbon additions on the high-temperature strength were conducted. High-temperature tensile tests in the temperature range 2500° to 4000° F and step-load creep tests at 3500° F were performed on swaged and annealed rod from these alloys.

#### EXPERIMENTAL PROCEDURE

The alloy systems studied fell into two groups: solid-solution-strengthened alloys (W-Hf, W-Ta-Re, W-Ta-Hf, W-Re-Hf, and W-Cb-Hf) and carbide-strengthened alloys (W-C, W-Cb-C, W-Ta-C, W-Ta-Re-C, and W-Hf-C). The compositions are given in table I. The alloys were prepared by consumable arc melting of pressed and sintered electrodes made from high-purity elemental tungsten and alloy addition powders. The basic features of the arc-melting furnace are described in reference 7. The majority of the alloys (indicated in table I) were melted onto a tungsten pad bolted to a retractable-water-cooled stool. As the ingot is formed, it is retracted so that melting occurs near the top of the mold and consequently with a greater exposure to the vacuum than is the case during deep-mold melting. The motions of the electrode and the stool were not coupled, allowing independent control of the two components. The remaining ingots were melted in the bottom of a deep, stationary mold which was progressively filled as the electrode melted. The residual gas pressure at the molten ingot top is several magnitudes higher with this technique compared with melting onto a retractable stool (ref. 8).

The alloys were fabricated into rod by extrusion and swaging, as indicated in table II. All the ingots were canned in molybdenum prior to extrusion. The cans were prepared by powder-metallurgy techniques and then machined to give a sliding fit with the billet. The cans were either 2 or 3 inches in diameter, and had wall thicknesses of 1/4 or 3/8 inch, respectively. The included angle on the nose of the can was 120°. The billets were induction heated in a hydrogen atmosphere and rapidly transferred to a conventional hydraulic press where they were extruded at a reduction ratio of 6 or 8 through zirconia coated steel dies. Total transfer extrusion time was less than 5 seconds in almost all cases, resulting in very little heat loss from the billets.

TABLE I. - ARC-MELTED TUNGSTEN ALLOYS

Alloy	Analyzed composition, atom percent  (a)	Interstitial contents, wt ppm			Ingot hardness (VHN) 10-kg load	Ingot microstructure  (b)
		Carbon	Nitrogen	Oxygen		
Unalloyed tungsten						
W-1	100 W	4	<5	2	351	SP
Tungsten-carbon						
C-1	0.12 C	78	8	5	414	TP
C-2	0.33 C	212	8	3	413	TP
C-3	0.93 C	668	<5	3	389	TP
Tungsten-columbium						
CB-1	<sup>c</sup> 2.25 Cb				---	SP
Tungsten-columbium-carbon						
CC-1	<sup>c</sup> 1.82 Cb - 0.005 C	3	<5	6	384	SP
CC-2	1.53 Cb - 0.008 C	5	24	3	378	SP
CC-3	0.51 Cb - 0.29 C	190	<5	2	411	TP
CC-4	0.44 Cb - 0.84 C	550	<5	3	408	TP
CC-5	0.75 Cb - 0.24 C	154	<5	11	419	TP
Tungsten-tantalum-carbon						
TC-1	<sup>c</sup> 1.32 Ta - 0.044 C	29	<5	2	397	TP
TC-2	<sup>c</sup> 2.67 Ta - 0.04 C	26	<5	6	---	TP
TC-3	0.43 Ta - 0.31 C	200	<5	2	385	TP
Tungsten-hafnium						
HF-1	0.21 Hf	3	<5	2	362	SP
HF-2	0.80 Hf	6	32	4	402	SP
HF-3	1.70 Hf	7	48	2	376	SP
Tungsten-hafnium-carbon						
HC-1	0.38 Hf - 0.015 C	10	<5	6	395	SP
HC-2	0.43 Hf - 0.07 C	46	<5	4	415	TP
HC-3	0.20 Hf - 0.26 C	171	10	<2	455	TP
Tungsten-tantalum-rhenium						
TR-1	0.98 Ta - 2.54 Re	3	<5	3	350	SP
TR-2	0.99 Ta - 4.70 Re	6	<5	7	322	SP
TR-3	2.72 Ta - 2.56 Re	3	<5	3	389	SP
TR-4	2.60 Ta - 4.20 Re	4	6	3	354	SP
Tungsten-tantalum-rhenium-carbon						
TRC-1	0.91 Ta - 2.53 Re - 0.005 C	3	<5	6	359	SP
TRC-2	1.00 Ta - 2.86 Re - 0.20 C	128	<5	7	365	TP
TRC-3	0.97 Ta - 2.62 Re - 0.92 C	600	6	7	---	TP
Tungsten-tantalum-hafnium						
TH-1	0.88 Ta - 0.31 Hf	4	<5	8	415	SP
TH-2	1.56 Ta - 0.40 Hf	2	<5	5	433	SP
Tungsten-columbium-hafnium						
CH-1	0.87 Cb - 0.35 Hf	5	<5	7	399	SP
CH-2	2.93 Cb - 0.42 Hf	<2	<5	4	395	SP
Tungsten-rhenium-hafnium						
RH-1	2.95 Re - 0.37 Hf	7	<5	4	332	SP
RH-2	4.77 Re - 0.36 Hf	5	<5	6	333	SP

<sup>a</sup> All ingots melted onto a retractable stool except where noted.<sup>b</sup> SP, single phase; TP, two phase.<sup>c</sup> Melted into a nonretractable deep mold.

TABLE II. - ALLOY FABRICATION CONDITIONS

Alloy	Extrusion temperature, °F	Reduction ratio	Breakthrough pressure, psi	Swaging temperature, °F	Swaging reduction, percent	Comments
Unalloyed tungsten						
W-1	3600	8	81 500	2300 to 2480	83	(a)
Tungsten-carbon						
C-1	3600	8	124 000	2550 to 2800	83	(a)
C-2	3600	8	133 000	2800 to 3100	83	(a)
C-3	4000	8	98 000	2850 to 3200	83	(a)
Tungsten-columbium						
CB-1	3500	8	143 700	2600 to 2740	74	(b)
Tungsten-columbium-carbon						
CC-1	4300	6	136 000	3260	79	(b)
CC-2	3800	8	77 200	2660 to 2850	83	(a)
CC-3	4000	8	121 000	3200 to 3250	85	(a)
CC-4	4000	8	117 000	3200 to 3300	85	(a)
CC-5	4000	8	122 000	3250 to 3300	85	(a)
Tungsten-tantalum-carbon						
TC-1	4000	8	128 700	2950 to 2980	64	(b)
TC-2	4000	8	172 600	3050 to 3100	64	(b)
TC-3	4000	8	114 000	2850 to 2950	85	(a)
Tungsten-hafnium						
HF-1	3600	8	110 000	2600 to 2800	83	(a)
HF-2	4000	8	103 000	2750 to 2950	83	(a)
HF-3	4000	8	144 000	3200	83	(a)
Tungsten-hafnium-carbon						
HC-1	4000	8	93 700	2600 to 2850	83	(a)
HC-2	4000	8	122 200	2800 to 3000	83	(a)
HC-3	4000	8	138 000	3200	85	(a)
Tungsten-tantalum-rhenium						
TR-1	4000	8	93 700	2600 to 2830	83	(a)
TR-2	4000	8	95 500	2630 to 2810	83	(a)
TR-3	4000	8	115 000	2720 to 2880	83	(a)
TR-4	4000	8	100 700	2900 to 2980	83	(a)
Tungsten-tantalum-rhenium-carbon						
TRC-1	3870	8	-----	2650 to 2820	83	(a)
TRC-2	3940	8	109 900	3050 to 3160	83	(a)
TRC-3	4100	8	114 100	3200 to 3300	83	(a)
Tungsten-tantalum-hafnium						
TH-1	4000	8	99 000	2850 to 3000	85	(a)
TH-2	4000	8	120 000	3100	85	(a)
Tungsten-columbium-hafnium						
CH-1	4000	8	109 000	2650 to 2850	85	(a)
CH-2	4000	8	110 000	2750 to 2900	85	(a)
Tungsten-rhenium-hafnium						
RH-1	4000	8	102 000	2850 to 2950	85	(a)
RH-2	4000	8	109 000	2870	85	(a)

<sup>a</sup> Extruded in 3-in.-diam molybdenum cans.<sup>b</sup> Extruded in 2-in.-diam molybdenum cans.

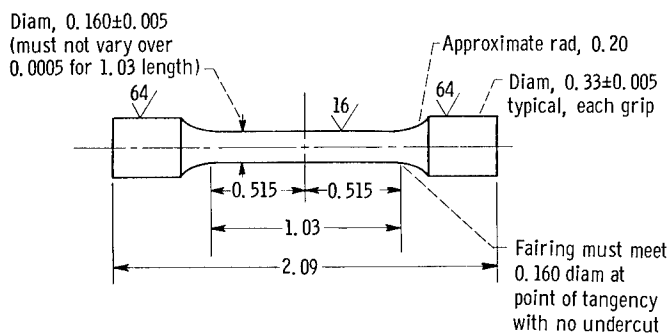


Figure 1. - Tensile and creep specimen. (All dimensions are in inches).

The extrusions were then cut and swaged with the molybdenum can intact, in most cases. This apparently improved the fabricability, since severe cracking was encountered on some alloys where the can was removed prior to swaging. The bars were induction heated in hydrogen and swaged approximately 10 percent per pass to the final size given in table II.

Complete details on the annealing and testing procedures are given in references 1 and 9. The tensile and creep specimen designs were identical (fig. 1) and had a 1-inch gage length and a 0.16-inch gage diameter. Tensile tests were performed in a vacuum of less than  $5 \times 10^{-5}$  torr at a constant crosshead speed of 0.05 inch per minute. The specimens were brought to temperature in approximately 1 hour and held at that temperature for 30 minutes prior to testing. Creep testing was performed in a beam-loaded unit equipped with a vacuum furnace similar to that employed for the tensile tests. The specimens were brought to temperature in  $1\frac{1}{2}$  to 2 hours and held at that temperature an equal amount of time prior to testing. During testing, the load was increased in steps so that the minimum creep rate could be measured for several stresses on the same specimen. Comparison tests showed that the creep rates measured in this manner are identical, within the limits of experimental error, to those measured by a series of single-load tests at 3500° F. Temperatures were measured with a W/W-26 Re thermocouple tied to the gage section. The thermocouple wire was calibrated by comparison with a calibrated optical pyrometer under blackbody conditions and is believed accurate to  $\pm 15^\circ$  F.

Specimens for light and electron microscopy were either mechanically or electrolytically polished. The etchants employed included boiling 3-percent hydrogen peroxide for the single-phase alloys and a lactic acid - hydrofluoric acid - nitric acid mixture for the two-phase alloys. Replicas for electron microscopy were made by a two-stage carbon-plastic technique shadowed with uranium dioxide.

## RESULTS

### (Consolidation and Fabrication)

A comparison is made in table III of the metallic and interstitial impurity analyses of a retractable-stool-melted ingot (W-1) with similar data on five lots of deep-mold-melted tungsten from reference 9. It is seen that the retractable-stool-melted material has a lower concentration of metallic impurities, while the interstitial impurities tend to be on the low side of the range indicated for the deep-mold-melted materials. The retractable-stool-melted materials are particularly lower in aluminum, iron, and silicon. This increase in purity is reflected in the lower recrystallization temperature of the wrought

TABLE III. - COMPARISON OF METALLIC AND INTERSTITIAL  
ANALYSES OF DEEP-MOLD AND RETRACTABLE-STOOL  
ARC-MELTED UNALLOYED TUNGSTEN

Element	Analyses <sup>a</sup>	
	Retractable stool (present study)	Deep mold (range of five lots) (ref. 9)
	Content, wt ppm	
Carbon	4	4-9
Nitrogen	5	8-13
Oxygen	2	2-6
Aluminum	<sup>b</sup> ND < 1	2-20
Calcium	ND < 1	ND < 10
Chromium	1	ND < 5-7
Copper	5	1-5
Iron	3	5-60
Manganese	ND < 1	ND < 1
Molybdenum	5	15
Sodium	ND < 1	ND < 10-20
Nickel	ND < 1	2-10
Silicon	ND < 1	5-15
Tin	ND < 1	ND < 5
Potassium	ND < 1	ND < 10-10

<sup>a</sup>Analyses on retractable-stool and deep-mold-melted tungsten obtained at different times from same commercial analytical laboratory. Note improved limits of detection in retractable-stool-melted analysis.

<sup>b</sup>Not detected, less than value noted.

Retractable-stool-melted materials. The latter material was 30 percent recrystallized after a 1-hour anneal at 2200° F, while similarly fabricated deep-mold-melted material recrystallized to this extent in the temperature range 2600° to 2900° F. (ref. 9).

An important parameter in the consolidation of arc-melted alloys is compositional control. With metallic additions, fairly consistent percentage losses due to vaporization during melting are encountered. These may be compensated for in the electrode composition. However, this is not the case with carbon additions. Figure 2 is a plot of the parts per million by weight of carbon added to an electrode against the amount retained in the ingot for several binary and ternary tungsten-metal-carbon systems. The carbon was added as spectrographic-grade graphite. The best retention was obtained for the binary tungsten-carbon alloys, as shown by the solid line. All the points for the other systems fell to the right of this line and are indicative of poorer retention of carbon during arc melting. This is attributed to the higher oxygen contents, which are probably present in the electrodes containing tantalum, columbium, hafnium, or rhenium powders. This higher oxygen content results in generally poorer compositional control in these materials compared



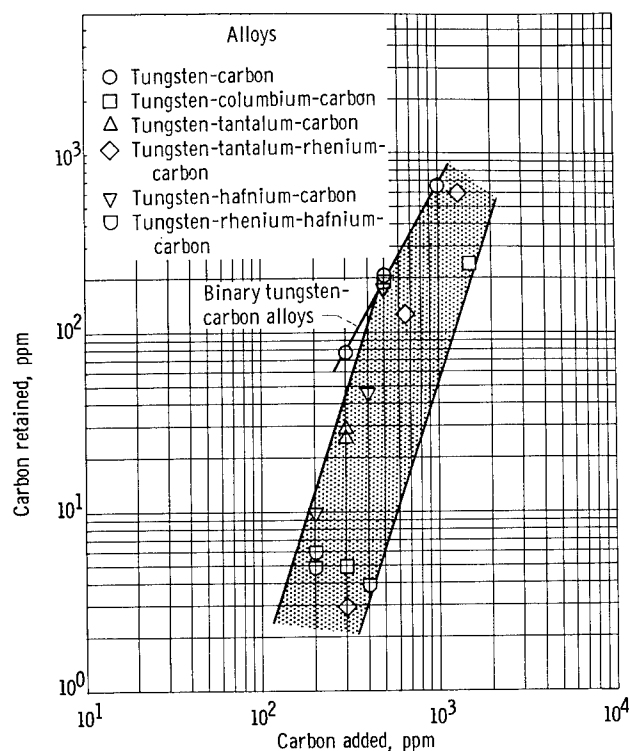


Figure 2. - Retention of carbon in various arc-melted tungsten alloy systems.

[with the binary W-C alloys since the carbon monoxide formed can be easily pumped off during melting.]

[These materials were canned in powder-metallurgy molybdenum prior to extrusion and swaging. Although no quantitative data were obtained on the relative extrudability of canned and uncanned tungsten alloys, it was found previously that the carbide-strengthened alloys could be extruded only at 4800° F when uncanned](ref. 1). [In the present work, canned alloys of this type could be easily extruded at 4000° F.]

### Ingot Microstructures

Table I gives data on the ingot microstructures and hardnesses. The solid-solution-strengthened alloys were all single phase, and the only significant feature of the microstructures was a coarse subgrain network in the large columnar grains. The alloys containing greater than 0.015 to 0.04 atom percent C (10 to 26 wt. ppm) were two phase; the second phase was presumably a metal carbide. Figure 3 shows typical as-melted microstructures from four of the carbon-containing alloy systems studied. The alloys in figure 3 have carbon contents of 0.26 to 0.33 atom percent and a metal addition of either tantalum, columbium, or hafnium. A binary W - 0.33 atom percent C alloy is included for comparison. Alloys of W-C, W-Cb-C, and W-Ta-C had similar microstructures and featured both grain boundary and globular intragranular particles. The W-Hf-C alloy, however, had plate-like intragranular particles in addition to the grain-boundary film. This may result from a limited interaction of the tantalum and

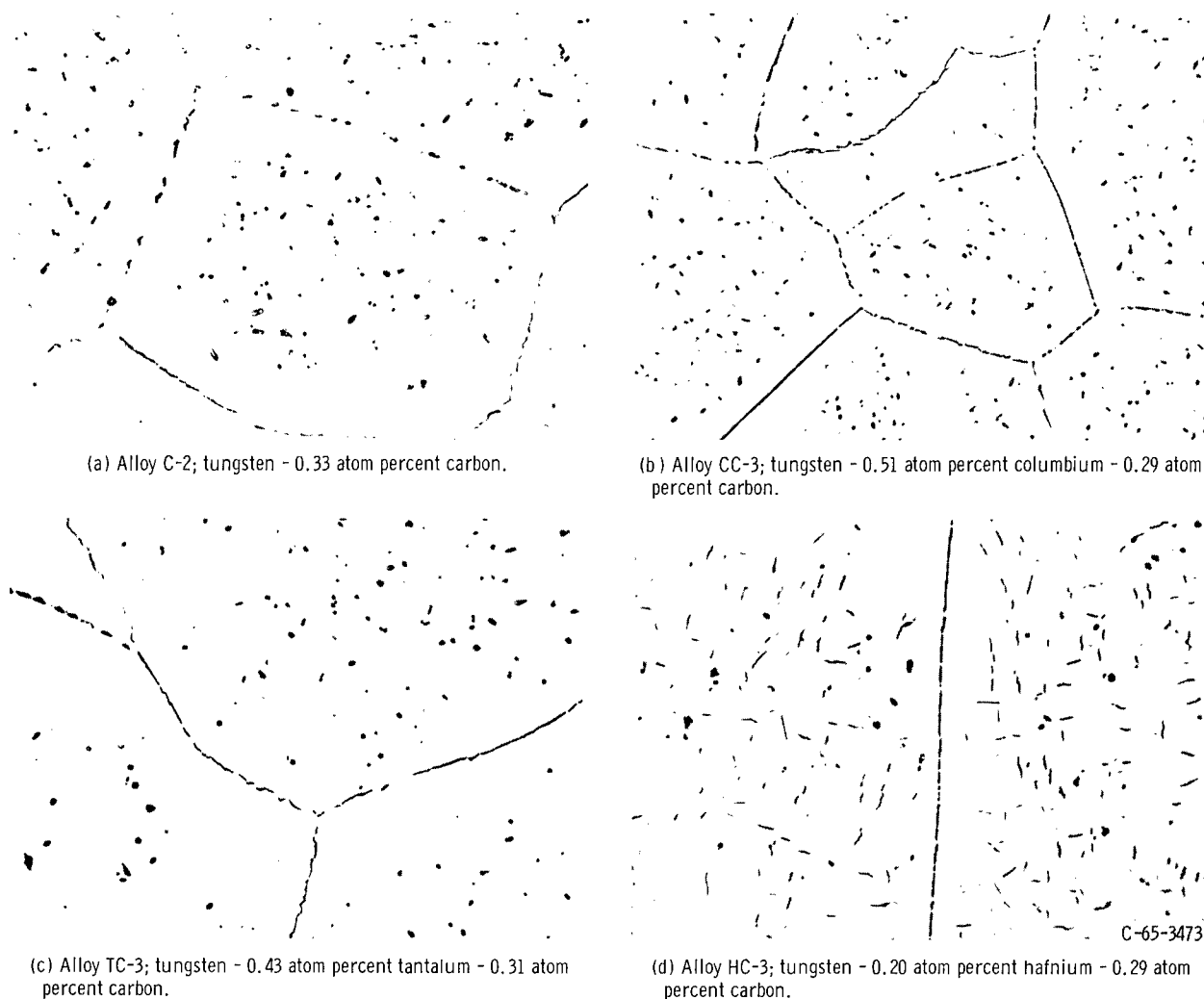


Figure 3. - Representative photomicrographs of four arc-melted carbon-containing tungsten alloys. As-melted condition; etchant, mixture of hydrofluoric, nitric, and lactic acids. X250. (Reduced 25 percent in printing.)

columbium with carbon and a strong interaction of hafnium with carbon resulting in the formation of hafnium carbide. Differences also were seen in the ingot hardnesses. The W - 0.20 atom percent Hf - 0.26 atom percent C alloy had a hardness of 455 compared with the hardnesses of 385 to 413 for other carbon-containing alloys under discussion.

#### Solid-Solution-Strengthened Alloys

[High-temperature tensile data on solid-solution-strengthened alloys are given in table IV.] [These alloy systems included W-Hf, W-Ta-Re, W-Cb-Hf, and W-Re-Hf. Data were obtained in both the as-swaged and recrystallized conditions. A standard recrystallization treatment of 3600° F for 1 hour was adopted for all the alloys.] The strengths in all the conditions are compared with average data on unalloyed arc-melted tungsten from reference 9.

→ p10

TABLE IV. - HIGH-TEMPERATURE TENSILE PROPERTIES OF SOLID-SOLUTION ALLOYS

[Composition in atom percent]

## (a) Tungsten-hafnium alloys

## (c) Tungsten-tantalum-hafnium alloys

Annealing conditions		Temperature, °F	0.2 Percent offset yield stress, psi	Ultimate tensile stress, psi	Elongation, percent	Reduction in area, percent
Time, hr	Temperature, °F					
HF-1, W - 0.21 Hf						
As-swaged		3000 3500 4000	----- 7.2x10 <sup>3</sup> 5.7	44.5x10 <sup>3</sup> 13.1 9.3	20 69 81	91 82 88
1	3600	2500 3000 3500	20.6x10 <sup>3</sup> ----- 7.39x10 <sup>3</sup>	32.4x10 <sup>3</sup> 23.7 13.5	24 28 75	>98 93 >98
HF-2, W - 0.80 Hf						
As-swaged		2500 3000 3500 4000	80.1x10 <sup>3</sup> 59.4 14.1 9.6	83.9x10 <sup>3</sup> 63.2 22.2 11.8	15 19 71 74	84 82 74 49
1	3600	2500 3000 3500	19.0x10 <sup>3</sup> 18.5 12.4	47.4x10 <sup>3</sup> 33.9 21.0	41 57 80	87 87 86
HF-3, W - 1.70 Hf						
As-swaged		3000 4000	50.3x10 <sup>3</sup> 13.2	81.0x10 <sup>3</sup> 15.1	28 (a)	78 (a)
1	3600	2500 3000 3500	32.7x10 <sup>3</sup> 25.3 20.6	63.4x10 <sup>3</sup> 44.9 30.4	32 (a) 44	82 (a) ---

## (b) Tungsten-tantalum-rhenium alloys

TR-1, W - 0.98 Ta - 2.54 Re						
As-swaged		3000	44.2×10 <sup>3</sup>	45.8×10 <sup>3</sup>	15	72
		3500	15.3	18.2	41	47
		4000	7.3	9.3	80	90
1	3600	2500	23.1×10 <sup>3</sup>	37.4×10 <sup>3</sup>	41	57
		3000	15.8	24.1	24	24
		3500	13.7	18.1	41	51
1	4200	3500	8.8×10 <sup>3</sup>	14.4×10 <sup>3</sup>	70	68
TR-2, W - 0.99 Ta - 4.70 Re						
As-swaged		3000	43.3×10 <sup>3</sup>	47.0×10 <sup>3</sup>	22	66
		3500	24.6	25.6	22	31
		4000	-----	8.8	80	71
1	3600	2500	26.6×10 <sup>3</sup>	40.9×10 <sup>3</sup>	26	28
		3000	13.8	23.0	20	18
		3500	10.4	15.2	36	28
1	4200	3500	9.1×10 <sup>3</sup>	14.6×10 <sup>3</sup>	60	53
TR-3, W - 2.72 Ta - 2.56 Re						
As-swaged		3000	46.0×10 <sup>3</sup>	48.1×10 <sup>3</sup>	20	55
		3500	25.3	25.9	11	21
		4000	7.9	9.9	56	39
1	3600	2500	27.3×10 <sup>3</sup>	45.3×10 <sup>3</sup>	49	76
		3000	19.0	27.1	26	59
		3500	15.9	19.8	36	49
1	4200	3500	10.7×10 <sup>3</sup>	16.5×10 <sup>3</sup>	30	34
TR-4, W - 2.60 Ta - 4.20 Re						
As-swaged		3000	53.0×10 <sup>3</sup>	54.7×10 <sup>3</sup>	26	84
		3500	-----	38.9	23	78
		4000	9.4×10 <sup>3</sup>	12.0	39	37
1	3600	2500	-----	57.4×10 <sup>3</sup>	36	95
		3000	-----	27.8	15	19
		3500	14.0×10 <sup>3</sup>	19.1	71	85
1	4200	3500	12.3×10 <sup>3</sup>	18.2×10 <sup>3</sup>	50	43

<sup>a</sup>Failed by splitting; no ductility values available.

Annealing conditions		Temperature, °F	0.2 Percent offset yield stress, psi	Ultimate tensile stress, psi	Elongation, percent	Reduction in area, percent
Time, hr	Temperature, °F					
		TH-1, W - 0.88 Ta - W.31 Hf				
As-swaged		3000	48.1x10 <sup>3</sup>	52.0x10 <sup>3</sup>	22	88
		3500	10.8	18.3	72	83
		4000	8.3	10.8	63	81
1	3600	2500	16.7x10 <sup>3</sup>	38.6x10 <sup>3</sup>	47	90
		3000	14.8	27.4	58	77
		3500	11.1	18.8	69	73
1	4000	3500	8.7x10 <sup>3</sup>	17.5x10 <sup>3</sup>	64	56
		TH-2, W - 1.56 Ta - 0.40 Hf				
As-swaged		3000	51.0x10 <sup>3</sup>	65.2x10 <sup>3</sup>	19	84
		3500	14.1	22.6	34	71
		4000	-----	10.4	57	42
1	3600	2500	19.3x10 <sup>3</sup>	41.6x10 <sup>3</sup>	49	92
		3000	17.6	33.7	41	66
		3500	13.7	21.9	61	40
1	4000	3500	-----	21.1x10 <sup>3</sup>	53	52

## (d) Tungsten-columbium-hafnium alloys

CH-1, W - 0.87 Cb - 0.35 Hf						
As-swaged		3000	49.7×10 <sup>3</sup>	51.6×10 <sup>3</sup>	23	84
		3500	12.6	19.2	91	77
		4000	8.4	10.8	67	49
1	3600	2500	19.8×10 <sup>3</sup>	40.0×10 <sup>3</sup>	48	94
		3000	14.0	28.0	55	77
		3500	11.8	18.9	67	64
1	4000	3500	10.6×10 <sup>3</sup>	17.7×10 <sup>3</sup>	61	49
CH-2, W - 2.93 Cb - 0.42 Hf						
As-swaged		3000	42.7×10 <sup>3</sup>	44.8×10 <sup>3</sup>	16	82
		4000	11.8	14.1	42	32
1	3600	2500	24.0×10 <sup>3</sup>	54.3×10 <sup>3</sup>	34	89
		3000	18.6	35.7	60	78
		3500	15.2	24.2	49	57
1	4000	3500	13.2×10 <sup>3</sup>	21.6×10 <sup>3</sup>	45	36

## (e) Tungsten-rhenium-hafnium alloys

RH-1, W - 2.95 Re - 0.37 Hf						
As-swaged		3000	59.6x10 <sup>3</sup>	63.7x10 <sup>3</sup>	19	80
		3500	17.6	19.6	79	76
		4000	-----	-----	--	--
1	3600	2500	22.1x10 <sup>3</sup>	49.0x10 <sup>3</sup>	54	91
		3000	18.7	33.1	70	90
		3500	13.5	18.6	54	66
1	4000	3500	12.6	19.3	89	68
RH-2, W - 4.77 Re - 0.36 Hf						
As-swaged		3000	55.7x10 <sup>3</sup>	62.6x10 <sup>3</sup>	30	86
		3500	13.7	19.6	77	62
		4000	8.9	10.4	65	42
1	3600	2500	23.0x10 <sup>3</sup>	51.7x10 <sup>3</sup>	45	95
		3000	19.0	33.4	60	90
		3500	13.1	18.8	76	59
1	4000	3500	-----	20.7x10 <sup>3</sup>	67	56

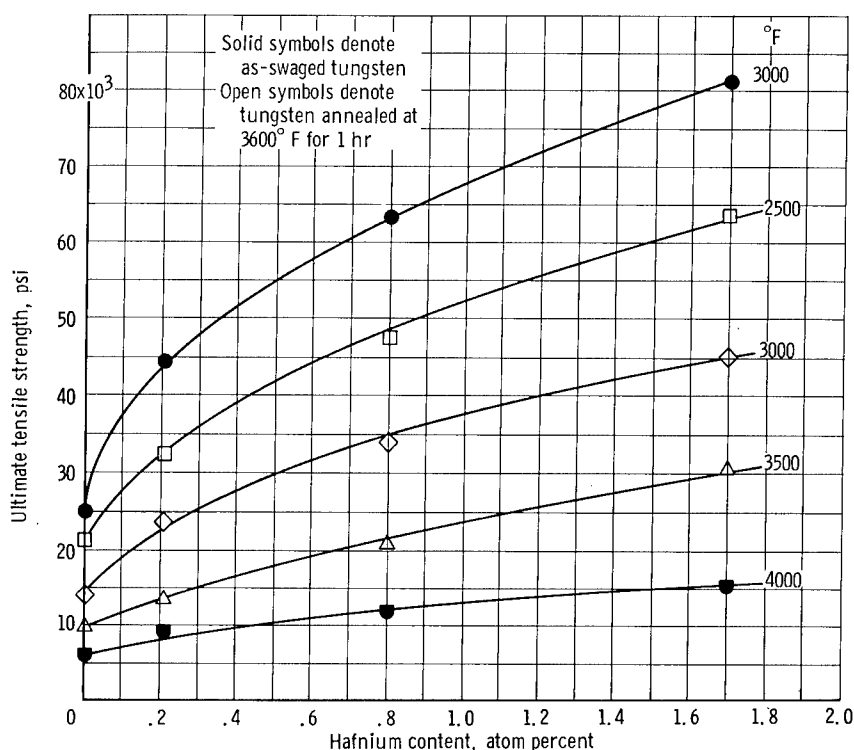


Figure 4. - Effect of hafnium on 2500° to 4000° F tensile strength of tungsten.

Figure 4 illustrates the effect of hafnium on the strength of tungsten at 2500° to 3500° F in the recrystallized condition and 3000° and 4000° F in the as-swaged condition. The alloys tested at 4000° F recrystallized during heating to the test temperature and thus can be considered to have been tested in the recrystallized condition. Considerable strengthening was achieved with the hafnium additions at all temperatures. For example, at 3000° F, the tensile strength of alloy HF-3, W - 1.7 atom percent Hf, was nearly three times that of unalloyed tungsten in the recrystallized condition. The as-swaged tensile strengths of these alloys at 3000° F also increased with hafnium content, reaching a value of 81 000 pounds per square inch at the 1.7 atom percent Hf level. At 3500° F, the as-swaged tensile strength is similar to that of the recrystallized material] (see table IV) [suggesting that the recrystallization temperature for these materials is below 3500° F.]

Tensile data for the W-Ta-Re ternary systems are given in table IV. An important feature of this alloy system is the retention of cold work during short-time tensile testing at 3500° F. For example, the tensile strength of alloy TR-4 (W - 2.60 atom percent Ta - 4.20 atom percent Re) was 19 100 pounds per square inch in the recrystallized condition and 38 900 pounds per square inch in the swaged condition. Similar but smaller differences between the as-swaged and recrystallized strengths were noted for the alloys TR-2 and TR-3. Metallographic examination of these alloys revealed wholly or partially cold-worked microstructures after tensile testing at 3500° F. Full recrystallization was noted, however, in all the as-swaged alloys after testing at 4000° F.

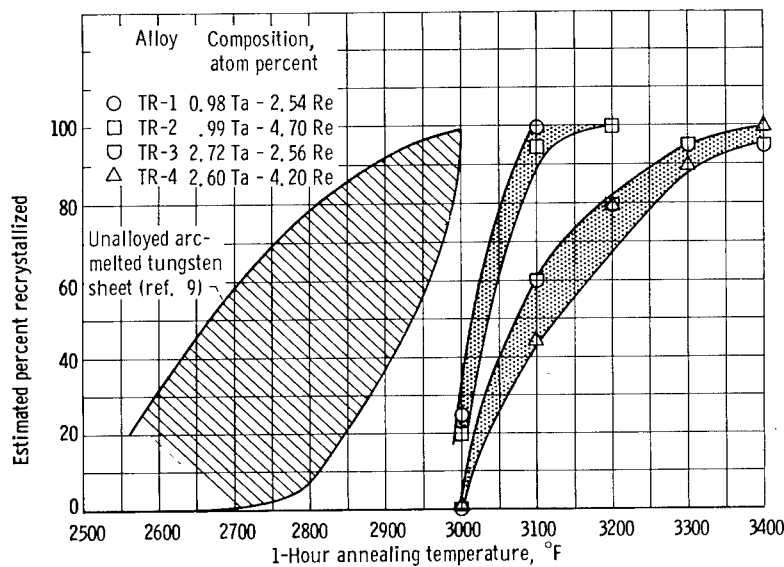


Figure 5. - Effect of tantalum and rhenium on recrystallization behavior of arc-melted tungsten sheet.

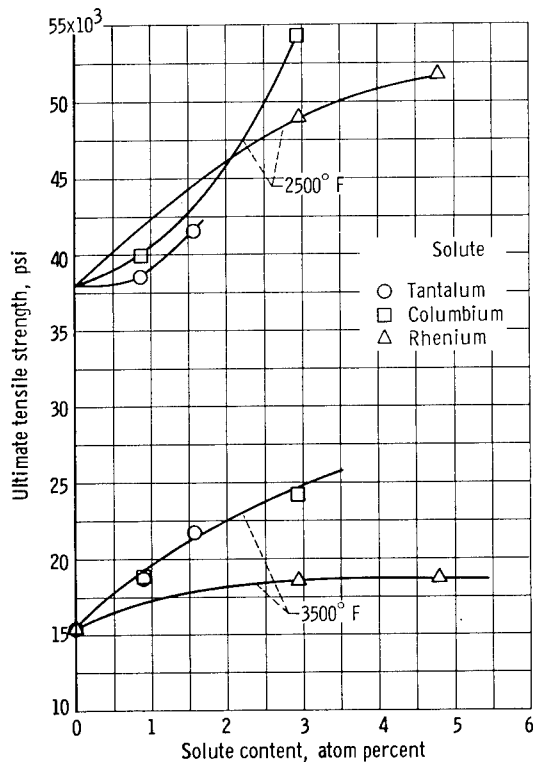


Figure 6. - Effect of tantalum, rhenium, and columbium on tensile strength of nominal tungsten - 0.37 atom percent hafnium alloy at 2500° and 3500° F in recrystallized condition.

The increased recrystallization temperatures in the W-Ta-Re system were studied further by annealing heavily worked sheet of the four W-Ta-Re alloys for 1 hour at temperatures of 2200° to 3400° F. Figure 5 is a plot of the percentage of the structure recrystallized as a function of the 1-hour annealing temperature for these materials. It is apparent that there is a large increase in recrystallization temperature induced by tantalum and rhenium, with tantalum evidently having the largest effect.

The strengths of the alloys in other ternary systems, W-Ta-Hf, W-Cb-Hf, and W-Re-Hf, are given in table IV. The influence of tantalum, columbium, and rhenium on the 2500° and 3500° F strength of recrystallized W - 0.37 atom percent Hf is illustrated in figure 6. The hafnium content represents the average hafnium content in the three systems (range 0.31 to 0.42 atom percent Hf) and its strength was interpolated from figure 4 (p. 10). Unlike the W-Ta-Re alloys, these latter three alloy systems did not show any cold-work strengthening at 3500° F; that is, the as-swaged and recrystallized tensile strengths were nearly identical. The strongest alloy

TABLE V. - CREEP OF SOLID-SOLUTION-STRENGTHENED ALLOYS AT 3500° F

[Composition in atom percent; all alloys annealed for 1 hr at 3600° F.]

## (a) Tungsten-hafnium alloys

Stress, psi	Minimum creep rate, $\dot{\epsilon}$ , sec <sup>-1</sup>
HF-1, W - 0.21 Hf	
3 060	$1.1 \times 10^{-7}$
3 700	$2.5 \times 10^{-7}$
4 470	$6.5 \times 10^{-7}$
5 370	$2.3 \times 10^{-6}$
6 380	$6.5 \times 10^{-6}$
7 400	$1.5 \times 10^{-5}$
HF-2, W - 0.80 Hf	
4 260	$1 \times 10^{-7}$
5 110	$2.5 \times 10^{-7}$
6 075	$6.8 \times 10^{-7}$
7 290	$1.4 \times 10^{-6}$
9 730	$8.5 \times 10^{-6}$
HF-3, W - 1.70 Hf	
6 320	$1.5 \times 10^{-7}$
7 580	$3.1 \times 10^{-7}$
9 100	$6.5 \times 10^{-7}$
10 880	$1.7 \times 10^{-6}$

## (b) Tungsten-tantalum-rhenium alloys

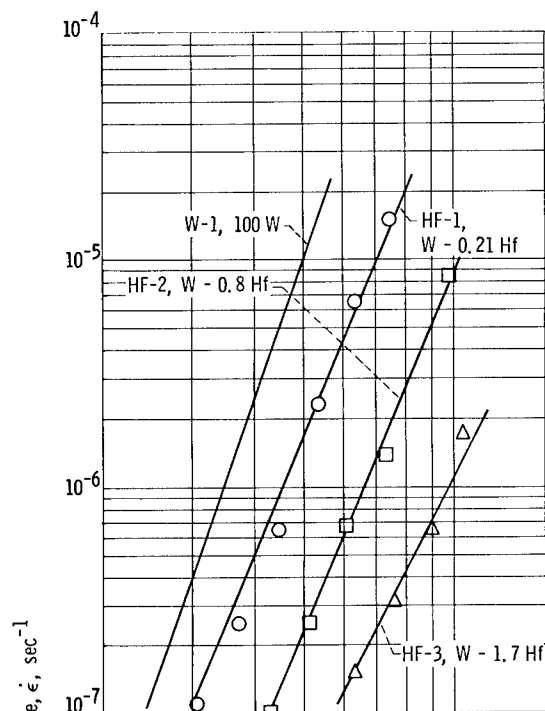
Stress, psi	Minimum creep rate, $\dot{\epsilon}$ , sec <sup>-1</sup>
TR-1, W - 0.98 Ta - 2.54 Re	
4440	$4.1 \times 10^{-7}$
5675	$1.8 \times 10^{-6}$
6910	$5 \times 10^{-6}$
TR-2, W - 0.99 Ta - 4.70 Re	
3290	$1.9 \times 10^{-7}$
4140	$7.4 \times 10^{-7}$
4990	$1.3 \times 10^{-6}$
5960	$5 \times 10^{-6}$
TR-3, W - 2.72 Ta - 2.56 Re	
6570	$4.1 \times 10^{-7}$
7800	$5.7 \times 10^{-6}$
9290	$2 \times 10^{-5}$
TR-4, W - 2.60 Ta - 4.20 Re	
5320	$3.2 \times 10^{-7}$
6430	$7.7 \times 10^{-7}$
7670	$2.7 \times 10^{-6}$
9150	$9.2 \times 10^{-6}$

## (c) Tungsten-tantalum-hafnium alloys

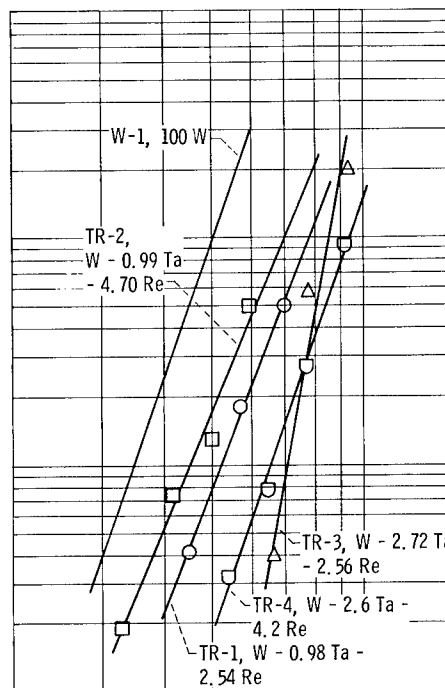
Stress, psi	Minimum creep rate, $\dot{\epsilon}$ , sec <sup>-1</sup>
TH-1, W - 0.88 Ta - 0.31 Hf	
4 360	$1.5 \times 10^{-7}$
5 570	$3.3 \times 10^{-7}$
6 790	$8.9 \times 10^{-7}$
8 000	$1.3 \times 10^{-6}$
9 450	$7.3 \times 10^{-6}$
10 900	$2.1 \times 10^{-5}$
TH-2, W - 1.56 Ta - 0.40 Hf	
5 025	$1.1 \times 10^{-7}$
6 185	$1.8 \times 10^{-7}$
7 500	$5.8 \times 10^{-7}$
10 600	$5.1 \times 10^{-6}$
11 860	$1.3 \times 10^{-5}$

## (d) Tungsten-rhenium-hafnium alloy

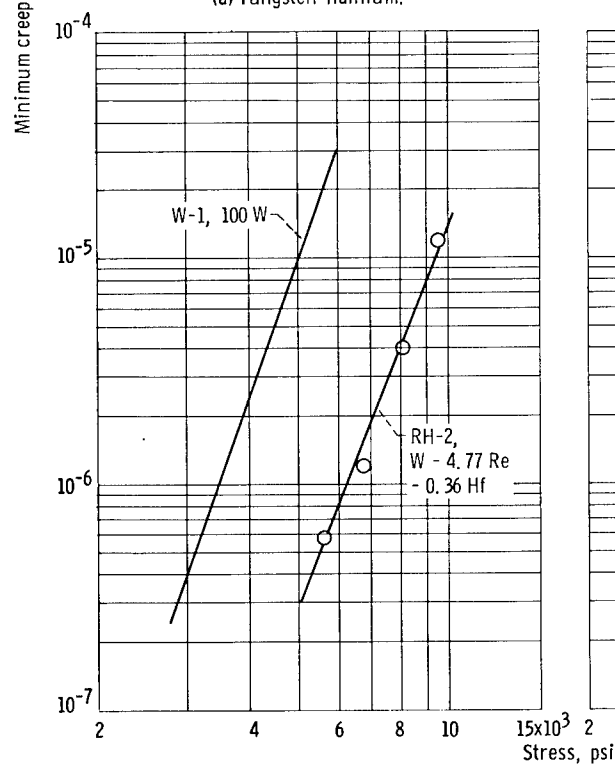
Stress, psi	Minimum creep rate, $\dot{\epsilon}$ , sec <sup>-1</sup>
RH-2, W - 4.77 Re - 0.36 Hf	
5610	$5.8 \times 10^{-7}$
6710	$1.2 \times 10^{-6}$
8050	$4 \times 10^{-6}$
9510	$1.2 \times 10^{-5}$



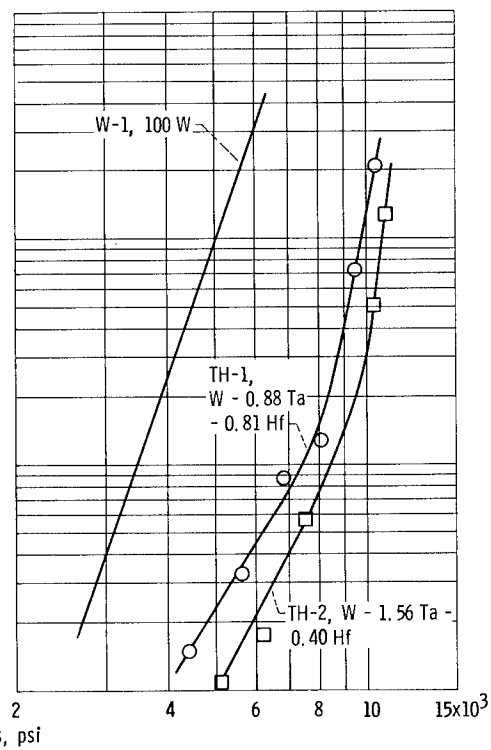
(a) Tungsten-hafnium.



(b) Tungsten-tantalum-rhenium.



(c) Tungsten-rhenium-hafnium.



(d) Tungsten-tantalum-hafnium.

Figure 7. - Creep behavior of solid-solution strengthened alloys at 3500° F (compositions in atom percent).

in this series was alloy CH-2, W - 2.93 atom percent Cb - 0.42 atom percent Hf, which had a strength of 24 200 pounds per square inch in the recrystallized condition at 3500° F. In addition, it is noted from figure 6 that tantalum and columbium are similar strengtheners at 3500° F.

Step-load creep tests were performed on several of the alloys in this series. The results are presented in table V and plotted in figure 7. Included for comparison are data obtained on unalloyed tungsten. All the creep tests were performed at 3500° F on material annealed for 1 hour at 3600° F.

For the majority of the alloys, the relation between the minimum (steady state) creep rate and stress was logarithmic, that is, of the form

$$\dot{\epsilon} = k\sigma^n$$

where  $\dot{\epsilon}$  is the minimum creep rate,  $\sigma$  is the applied stress, and  $k$  and  $n$  are constants. A least-squares analysis of the curves in figure 7 produced values of  $n$  ranging from 4.4 to 11.2, with the majority of the values falling between 5 and 6. There was no consistent dependence of  $n$  on alloy content. These values may be compared with the value of 5.8 for unalloyed arc-melted tungsten (ref. 9). Only in the case of the W-Ta-Hf alloys (fig. 7(d)) did this empirical relation not hold. For these alloys, a bend in the plot was noted at a minimum creep rate of approximately  $10^{-6}$  per second.

The same general order of strengthening found in the tensile tests was evidenced in the creep tests with hafnium additions being the most effective and rhenium the least effective.

In reference 1, it was suggested that the alloying elements can also strengthen to some degree by interaction with unintentionally added interstitial impurities. This effect was examined in creep by testing alloy CB-1 (W - 2.25 atom percent Cb) at 3500° F after three different annealing treatments designed to alter the extent of this interaction. The treatments were

- (1) 4000° F for 1 hour, slow cooled (approximately 12° F/min)
- (2) 4000° F for 1 hour, helium quenched (approximately 500° F/sec)
- (3) 3600° F for 1 hour, normal furnace cooled (approximately 200° F/min)

The results are given in table VI and plotted in figure 8. As shown in figure 8, there is a difference in the creep rate at a given stress for each condition. Of the two specimens annealed at 4000° F, the highest creep strength<sup>1</sup> was obtained on the helium-quenched material. The creep strength for this material was approximately 5400 pounds per square inch, while that of the slowly cooled specimen was 4800 pounds per square inch. Thus, the faster cooling rate produces the higher creep strength. Metallographic examination of these specimens annealed at 4000° F showed a globular precipitate at the grain boundaries

---

<sup>1</sup>Creep strength will be defined throughout as the interpolated stress at a minimum creep rate of  $10^{-6}$  sec<sup>-1</sup>.



TABLE VI. - EFFECT OF HEAT TREATMENT ON CREEP

PROPERTIES OF ALLOY CB-1; TUNGSTEN -  
2.25 ATOM PERCENT COLUMBIUM

Stress, psi	Minimum creep rate, $\dot{\epsilon}$ , $\text{sec}^{-1}$
Annealed 1 hr at 4000° F; slow cooled	
4310	$4.9 \times 10^{-7}$
5270	$1.7 \times 10^{-6}$
6210	$6.3 \times 10^{-6}$
7420	$2.9 \times 10^{-5}$
Annealed 1 hr at 4000° F; helium quenched	
4480	$3.9 \times 10^{-7}$
4980	$6.5 \times 10^{-7}$
5720	$1.2 \times 10^{-6}$
6470	$2.4 \times 10^{-6}$
Annealed 1 hr at 3600° F; normal cooled	
3660	$1.3 \times 10^{-7}$
4150	$2.3 \times 10^{-7}$
5610	$1.2 \times 10^{-6}$
6340	$2.6 \times 10^{-6}$
7200	$5.8 \times 10^{-6}$
8050	$1.2 \times 10^{-5}$

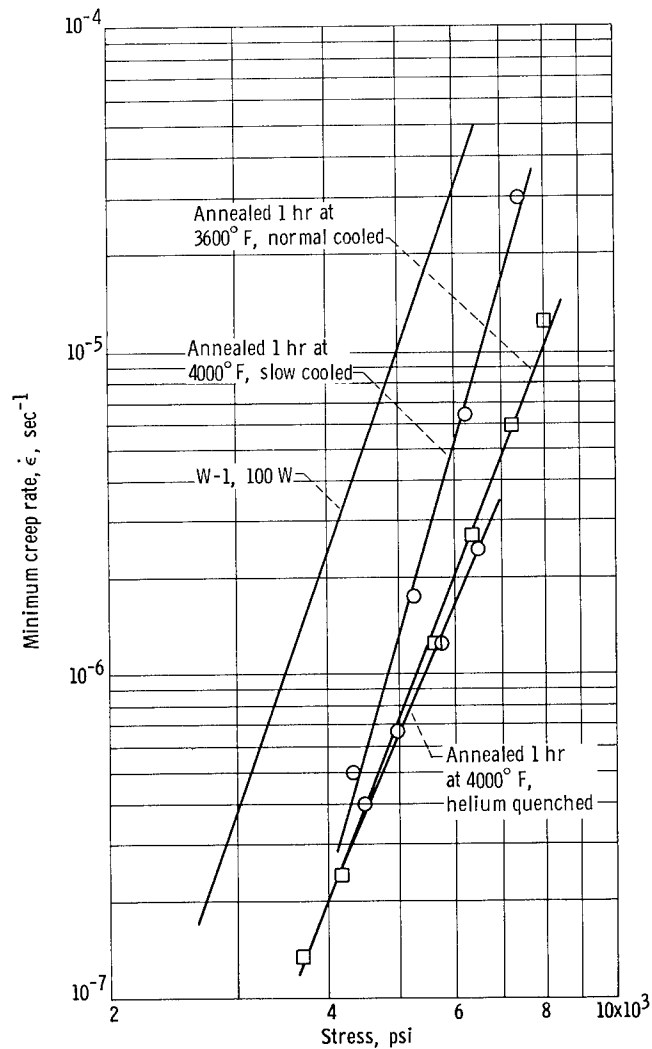


Figure 8. - Creep of alloy CB-1, tungsten - 2.25 atom percent columbium, at 3500° F after three different annealing treatments.

of the slowly cooled material, but none in the quenched specimen. The oxygen and carbon contents were nearly identical, although reliable nitrogen analyses were not available. The creep strength of the material annealed at 3600° F was approximately the same as that of condition (2).

### Carbide-Strengthened Alloys

The influence of carbon additions on the high-temperature strength of unalloyed tungsten and W-Cb, W-Ta, W-Ta-Re, and W-Hf alloys was studied. The tensile data are presented in table VII and plotted as a function of test temperature in figures 9 to 13.

Figure 9 illustrates the effect of temperature on the strength of binary tungsten-carbon alloys containing 0.12 to 0.93 atom percent C. It is of

TABLE VII. - TENSILE PROPERTIES OF CARBIDE-STRENGTHENED ALLOYS

[Composition in atom percent.]

## (a) Tungsten-carbon alloys

Annealing conditions		Temperature, °F	0.2 Percent offset yield stress, psi	Ultimate tensile stress, psi	Elongation, percent	Reduction in area, percent
Time, hr	Temperature, °F					
C-1, W - 0.12 C						
As-swaged		3000 4000	22.0×10 <sup>3</sup> 1.6	23.3×10 <sup>3</sup> 6.56	30 87	>98 >98
1	3600	2500 3000 3500	9.5×10 <sup>3</sup> 7.2 3.0	19.7×10 <sup>3</sup> 12.5 7.4	69 76 76	>98 >98 >98
C-2, W - 0.33 C						
As-swaged		3000 3500	60.6×10 <sup>3</sup> 9.8	69.3×10 <sup>3</sup> 16.2	14 70	75 >98
1	3600	2500 3000 3500	10.4×10 <sup>3</sup> 6.2 4.6	20.6×10 <sup>3</sup> 15.0 9.2	67 57 68	>98 >98 >98
C-3, W - 0.93 C						
As-swaged		3000 3500 4000	59.1×10 <sup>3</sup> 7.2 3.8	61.8×10 <sup>3</sup> 11.1 6.91	24 71 92	86 >98 >98
1	3600	2500 3000 3500	16.6×10 <sup>3</sup> 11.3 6.6	29.6×10 <sup>3</sup> 18.4 10.0	73 65 75	>98 >98 >98

## (b) Tungsten-tantalum-carbon alloys

TC-1, W - 1.32 Ta - 0.04 C						
As-swaged		3500	7.5×10 <sup>3</sup>	15.0×10 <sup>3</sup>	50	>98
1	3600	3500	8.8×10 <sup>3</sup>	14.9×10 <sup>3</sup>	71	94
	4200	31.00	7.8	15.4	77	85
TC-2, W - 2.67 Ta - 0.04 C						
1	3600	3500	12.4×10 <sup>3</sup>	21.6×10 <sup>3</sup>	69	95
TC-3, W - 0.43 Ta - 0.31 C						
As-swaged		3000 3500 4000	75.0×10 <sup>3</sup> 11.0 3.4	84.0×10 <sup>3</sup> 16.6 8.2	20 72 88	68 >98 >98
1	3600	2500	19.2×10 <sup>3</sup>	48.7×10 <sup>3</sup>	51	90
		3000	17.3	32.7	68	93
		3500	10.4	16.5	106	>98

## (c) Tungsten-columbium-carbon alloys

CC-1, W - 1.82 Cb - 0.005 C						
As-swaged		3000 3500	39.3×10 <sup>3</sup> 13.3	43.2×10 <sup>3</sup> 16.9	9 43	39 95
1	3600	2500	29.3×10 <sup>3</sup>	36.5×10 <sup>3</sup>	22	95
		3000	17.0	21.1	---	---
		3500	7.3	12.5	28	35
		4000	6.1	8.2	93	>98
1	4200	3000 3500	10.6×10 <sup>3</sup> 8.3	20.5×10 <sup>3</sup> 14.2	58 69	94 91
		CC-2, W - 1.53 Cb - 0.008 C				
As-swaged		2500 3000 3500 4000	55.5×10 <sup>3</sup> 46.5 10.0 6.2	65.9×10 <sup>3</sup> 47.9 16.5 8.9	13 18 77 59	31 91 >98 49
1	3600	2500 3000 3500	22.6×10 <sup>3</sup> 10.1 8.3	38.2×10 <sup>3</sup> 25.5 13.5	46 49 59	>98 >98 58
		CC-3, W - 0.51 Cb - 0.29 C				
		1	3600	2500 3500	25.5×10 <sup>3</sup> 16.1	32.2×10 <sup>3</sup> 20.8
CC-4, W - 0.44 Cb - 0.84 C						
1	3600	2500 3000 3500	33.0×10 <sup>3</sup> 22.6 15.2	63.0×10 <sup>3</sup> 43.3 22.5	39 57 56	86 85 >98
		CC-5, W - 0.75 Cb - 0.24 C				
		1	3600	2500 3000 3500	35.3×10 <sup>3</sup> 28.7 15.1	73.1×10 <sup>3</sup> 45.8 21.8

## (d) Tungsten-tantalum-rhenium-carbon-alloys

Annealing conditions		Temperature, °F	0.2 Percent offset yield stress, psi	Ultimate tensile stress, psi	Elongation, percent	Reduction in area, percent
Time, hr	Temperature, °F					
TRC-1, W - 0.91 Ta - 2.53 Re - 0.005 C						
As-swaged		3000 3500 4000	42.1×10 <sup>3</sup> 8.4 6.5	43.9×10 <sup>3</sup> 14.9 8.6	22 50 82	76 42 81
1	3600	2500	20.3×10 <sup>3</sup>	38.3×10 <sup>3</sup>	--	---
		3000	17.1	26.0	40	56
		3500	10.3	15.4	68	60
1	4200	3500	8.6×10 <sup>3</sup>	14.0	80	80
TRC-2, W - 1.00 Ta - 2.86 Re - 0.20 C						
As-swaged		3000 3500 4000	63.4×10 <sup>3</sup> 12.2 6.1	66.8×10 <sup>3</sup> 18.7 8.8	20 67 --	75 >98 ---
1	3600	2500	27.4×10 <sup>3</sup>	66.3×10 <sup>3</sup>	37	82
		3000	25.0	37.6	62	73
		3500	12.3	17.4	70	>98
TRC-3, W - 0.97 Ta - 2.62 Re - 0.02 C						
As-swaged		3000 3500 4000	70.1×10 <sup>3</sup> 20.4 9.4	85.3×10 <sup>3</sup> 25.7 12.8	17 71 45	59 90 >98
1	3600	2500	45.0×10 <sup>3</sup>	80.8×10 <sup>3</sup>	41	80
		3000	31.0	57.2	56	84
		3500	15.9	23.2	67	90
1	4200	3500	16.7×10 <sup>3</sup>	22.7×10 <sup>3</sup>	51	72

## (e) Tungsten-hafnium-carbon alloys

HC-1, W - 0.26 Hf - 0.015 C						
As-swaged		2500	68.3x10 <sup>3</sup>	84.2x10 <sup>3</sup>	15	83
		3000	59.3	62.0	15	86
		3500	17.0	18.4	82	>98
		4000	7.2	10.0	86	82
1	3600	2500	22.0x10 <sup>3</sup>	47.6x10 <sup>3</sup>	20	91
		3000	21.5	32.0	--	---
		3500	10.3	19.0	76	81
HC-2, W - 0.52 Hf - 0.09 C						
As-swaged		3000	58.7x10 <sup>3</sup>	66.6x10 <sup>3</sup>	20	86
1	3600	2500	34.9x10 <sup>3</sup>	55.1x10 <sup>3</sup>	27	>98
		3000	28.8	50.5	31	87
		3500	21.3	26.6	52	81
		3500	-----	27.3	50	90
		4000	12.2x10 <sup>3</sup>	14.7	35	84
HC-3, W - 0.20 Hf - 0.26 C						
As-swaged		3000	60.4x10 <sup>3</sup>	88.2x10 <sup>3</sup>	16	86
		3500	57.1	62.5	17	83
4	4200	3500	28.6x10 <sup>3</sup>	35.6x10 <sup>3</sup>	30	86

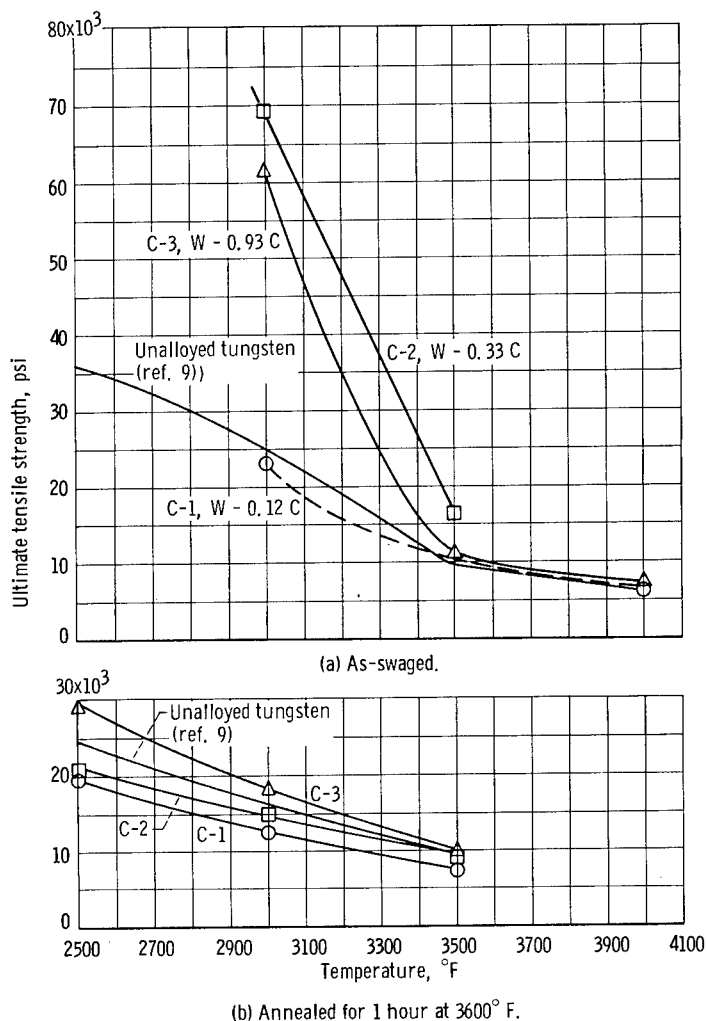


Figure 9. - Tensile properties of tungsten-carbon alloys (compositions in atom percent).

particular interest to note that the strength of the W - 0.12 and W - 0.33 atom percent C alloys in the recrystallized condition was lower than that of unalloyed tungsten, while the W - 0.93 atom percent C alloy was stronger. This reduction in high-temperature strength by the carbon additions occurs in spite of the considerable amount of carbide precipitate found in these materials, as will be illustrated later.

Figure 10 shows the strength of a W-Ta-C alloy as a function of temperature. Data at 3500° F on two additional W-Ta-C alloys are given in table VII. The alloy TC-3 had a particularly high strength, 84 100 pounds per square inch, in the swaged condition at 3000° F. The strength of this alloy, however, decreased sharply to 16 600 pounds per square inch at 3500° F.

The strengths of the W-Cb-C alloys shown in figure 11 could be divided into two groups: CC-1 and CC-2 containing 0.005 and 0.008 atom percent C, respectively, and CC-3, CC-4, and CC-5, which contained 0.24 to 0.84 atom

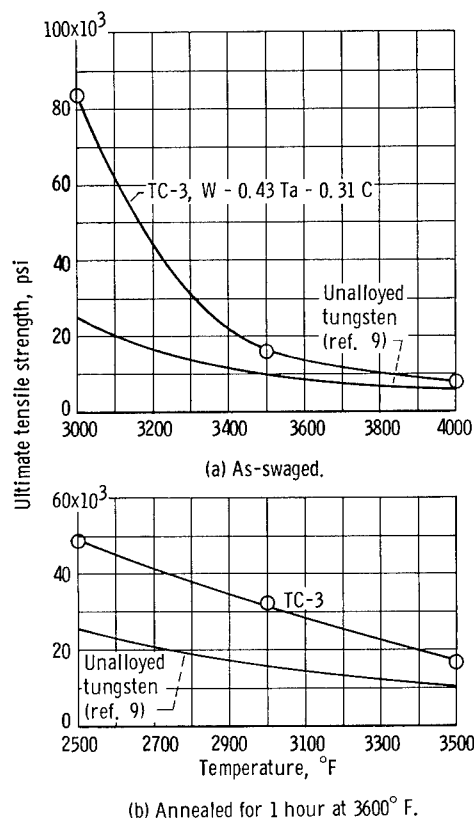


Figure 10. - Tensile properties of tungsten-tantalum-carbon alloys (compositions in atom percent).

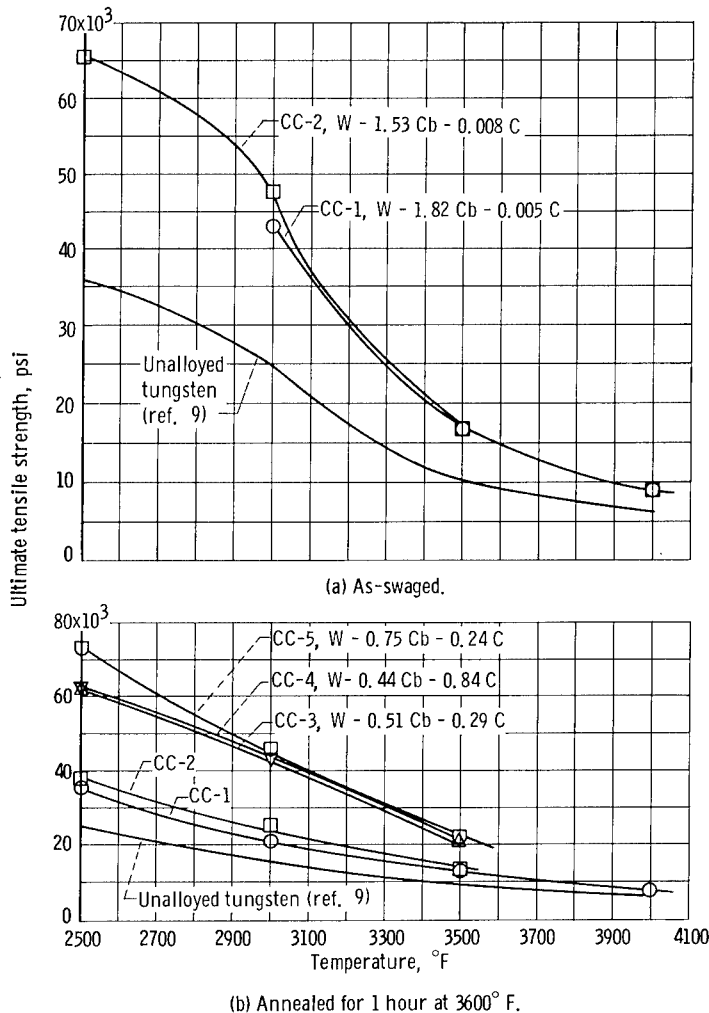


Figure 11. - Tensile properties of tungsten-columbium-carbon alloys (compositions in atom percent).

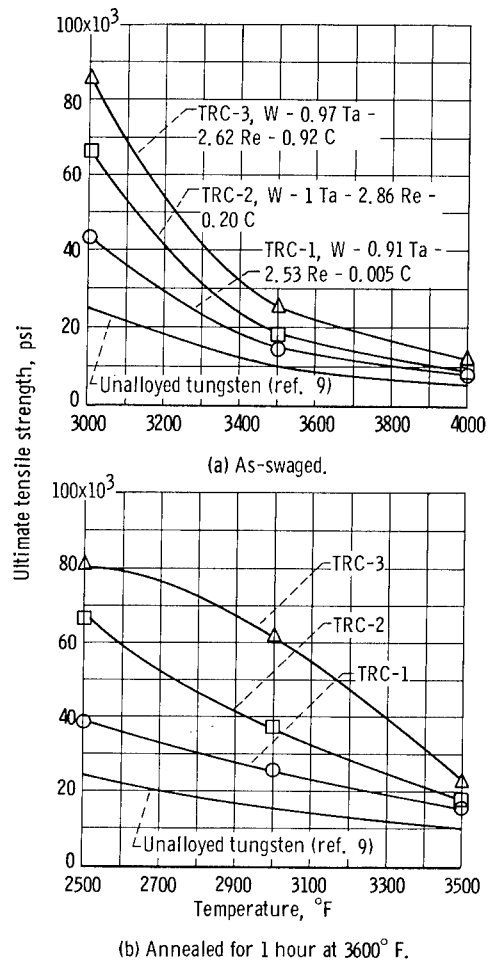


Figure 12. - Tensile properties of tungsten-tantalum-rhenium-carbon alloys (compositions in atom percent).

percent C. In the recrystallized condition, low carbon alloys were slightly stronger than unalloyed tungsten, while the high carbon alloys had strengths approximately 170 to 200 percent higher than those of unalloyed tungsten at all temperatures.

Figure 12 shows the influence of carbon on the strength of a nominal W - 1-atom-percent Ta - 3 atom percent Re alloy. The strength of these alloys increased continuously with increasing carbon content, both in the swaged and recrystallized conditions. Alloy TRC-3, W - 0.97 atom percent Ta - 2.62 atom percent Re - 0.92 atom percent C, had a strength of 85 300 pounds per square inch at 3000° F in the swaged condition, the strength decreasing to 25 700 pounds per square inch at 3500° F. This is not as large a drop in strength as that found in the W-Ta-C alloy, shown in figure 10, even though the strengths at 3000° F were nearly identical.

The highest strengths obtained in the carbon containing alloy systems were

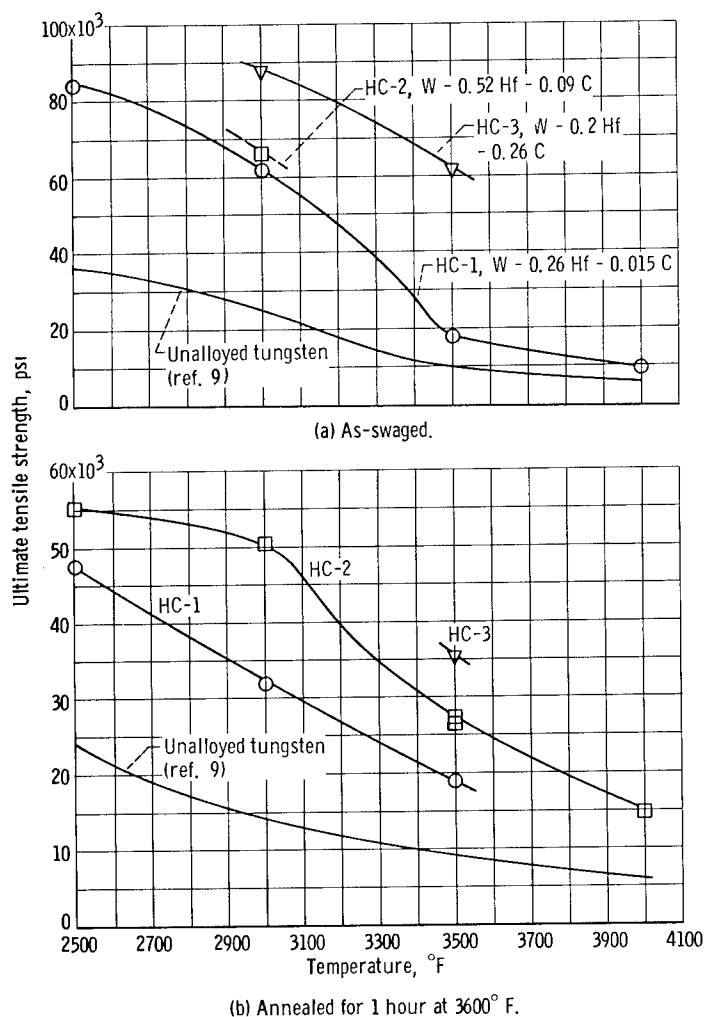


Figure 13. - Tensile properties of tungsten-hafnium-carbon alloys (compositions in atom percent).

in the W-Hf-C alloy, the data for which are plotted in figure 13. An outstanding characteristic of these alloys is the stability of the cold-worked structure at 3500° F. To the authors' knowledge, the strength level in swaged specimens of alloy HC-3, W - 0.2 atom percent Hf - 0.26 atom percent C, was the highest ever reported for a metallic material at these temperatures. The strengths were 88 200 and 62 500 pounds per square inch at 3000° and 3500° F, respectively. The latter value is more than six times that of unalloyed tungsten at this temperature. Metallographic examination showed no trace of recrystallization after testing at 3500° F. In addition, alloy HC-2, W - 0.52 atom percent Hf - 0.09 atom percent C was only about 60 percent recrystallized after annealing at 3600° F and testing at 3500° F. Alloy HC-3 was fully recrystallized only after heating for 4 hours at 4200° F. At 3500° F, the strength of this recrystallized alloy was 35 600 pounds per square inch, higher than that of any other recrystallized material tested in this program.

Creep strengths for these alloys at 3500° F are given in figure 14 and tabulated in table VIII. In general, the relative tensile strengths of the alloys were also reflected in the creep strengths. The creep strength of the binary W-C alloys was nearly the same or lower than that of unalloyed tungsten (fig. 14(a)). The W-Cb-C alloys had approximately the same degree of strength improvement as in the tensile tests (fig. 11). Creep strengths of the W-Ta-C alloys shown in figure 14(c), depended more on tantalum content than carbon content. For example, the creep strength of TC-2, W - 2.67 atom percent Ta - 0.04 atom percent C, was 6400 pounds per square inch, while that of TC-3, W - 0.43 atom percent Ta - 0.31 atom percent C, was 3800 pounds per square inch. Data for two W-Hf-C alloys are given in figure 14(d). The creep strength at 3500° F of recrystallized HC-3, W - 0.20 atom percent Hf - 0.26 atom percent C, was 8000 pounds per square inch compared with 6400 pounds per square inch for HC-2, W - 0.43 atom percent Hf - 0.07 atom percent C. The ratio of these two values is nearly the same as the ratio of the recrystallized tensile strengths of these alloys at this temperature, as indicated previously in figure 13.

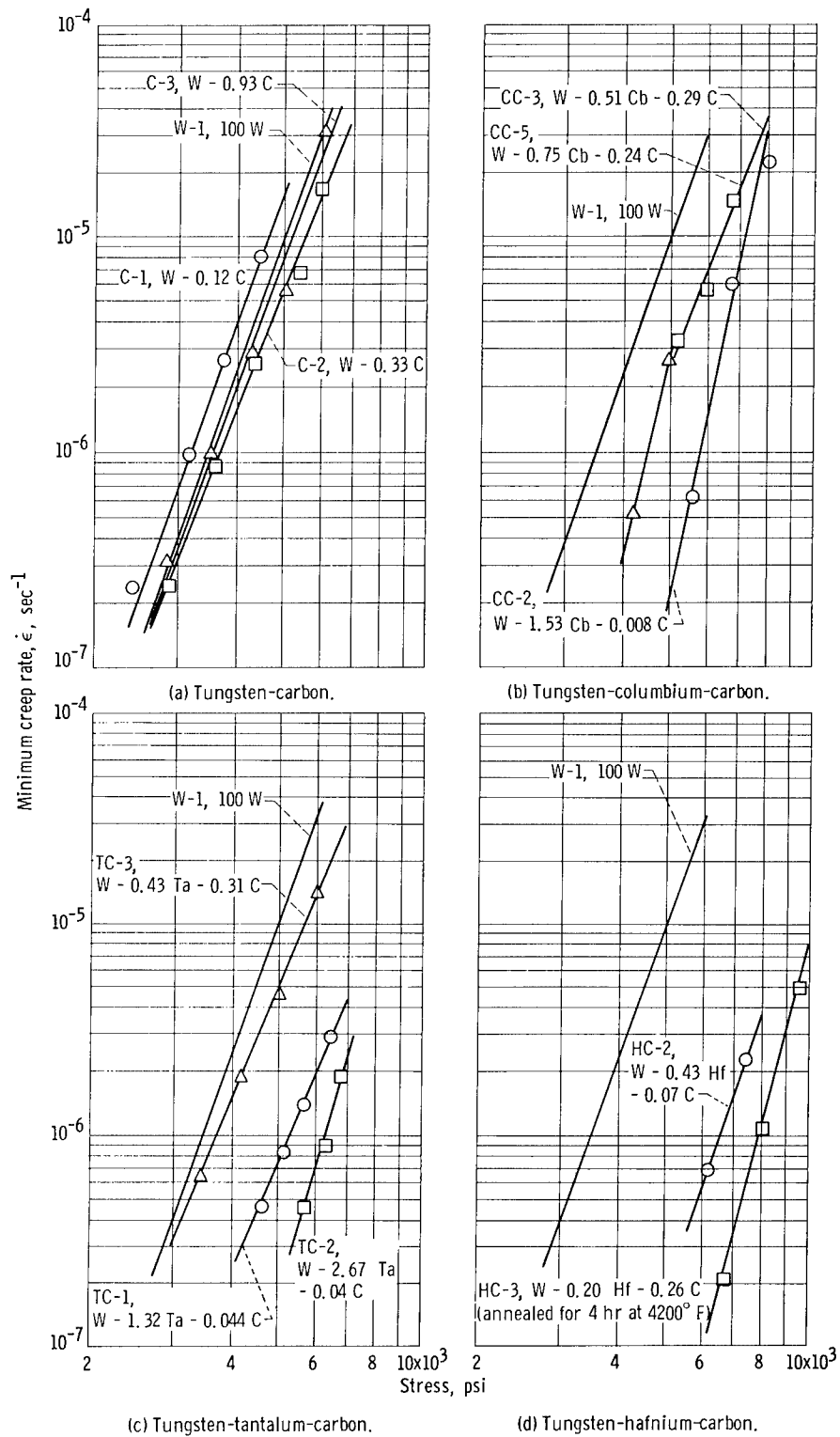


Figure 14. - Creep behavior of carbide-strengthened alloys at 3500° F (compositions in atom percent).

TABLE VIII. - CREEP OF CARBIDE-STRENGTHENED ALLOYS AT 3500° F

[Composition in atom percent; all alloys  
annealed for 1 hr at 3600° F.]

## (a) Tungsten-carbon alloys

Stress, psi	Minimum creep rate, $\dot{\epsilon}$ , sec <sup>-1</sup>
C-1, W - 0.12 C	
2480	$2.4 \times 10^{-7}$
3150	$1 \times 10^{-6}$
3720	$2.7 \times 10^{-6}$
4470	$8.1 \times 10^{-6}$
C-2, W - 0.33 C	
2875	$2.4 \times 10^{-7}$
3590	$8.8 \times 10^{-7}$
4320	$2.6 \times 10^{-6}$
5390	$6.9 \times 10^{-6}$
5990	$1.7 \times 10^{-5}$
C-3, W - 0.93 C	
2850	$3.2 \times 10^{-7}$
3500	$1 \times 10^{-6}$
4270	$2.9 \times 10^{-6}$
5050	$5.7 \times 10^{-6}$
6085	$3.2 \times 10^{-5}$

## (c) Tungsten-tantalum-carbon alloys

Stress, psi	Minimum creep rate, $\dot{\epsilon}$ , sec <sup>-1</sup>
TC-1, W - 1.32 Ta - 0.044 C	
4620	$5.2 \times 10^{-7}$
5130	$8.3 \times 10^{-7}$
5630	$1.4 \times 10^{-6}$
6420	$2.9 \times 10^{-6}$
TC-2, W - 2.67 Ta - 0.04 C	
5660	$4.6 \times 10^{-7}$
6270	$8.9 \times 10^{-7}$
6760	$1.9 \times 10^{-6}$
TC-3, W - 0.43 Ta - 0.31 C	
3420	$6.4 \times 10^{-7}$
4150	$1.9 \times 10^{-6}$
5010	$4.6 \times 10^{-6}$
5990	$1.4 \times 10^{-5}$

## (b) Tungsten-columbium-carbon alloys

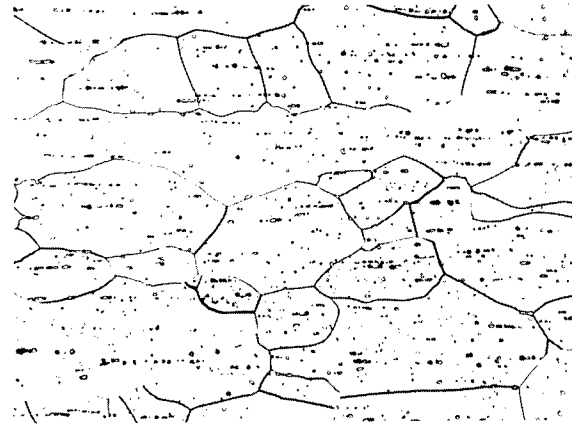
Stress, psi	Minimum creep rate, $\dot{\epsilon}$ , sec <sup>-1</sup>
CC-2, W - 1.53 Cb - 0.008 C	
5560	$6.3 \times 10^{-7}$
6700	$6.1 \times 10^{-6}$
8000	$2.3 \times 10^{-5}$
CC-3, W - 0.51 Cb - 0.29 C	
5185	$3.3 \times 10^{-6}$
5960	$5.7 \times 10^{-6}$
6740	$1.5 \times 10^{-5}$
CC-5, W - 0.75 Cb - 0.24 C	
4190	$5.3 \times 10^{-7}$
4970	$2.7 \times 10^{-6}$

## (d) Tungsten-hafnium-carbon alloys

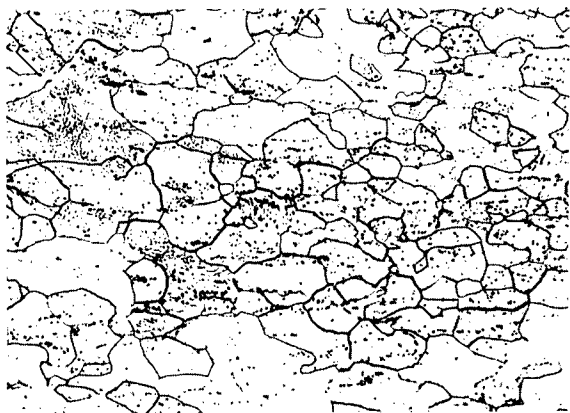
Stress, psi	Minimum creep rate, $\dot{\epsilon}$ , sec <sup>-1</sup>
HC-2, W - 0.43 Hf - 0.07 C	
6140	$7 \times 10^{-7}$
7370	$2.3 \times 10^{-6}$
HC-3, W - 0.20 Hf - 0.26 C	
6630	$2.1 \times 10^{-7}$
7950	$1.1 \times 10^{-6}$
9550	$5 \times 10^{-6}$



(a) Alloy CB-2; tungsten - 1.53 atom percent columbium.



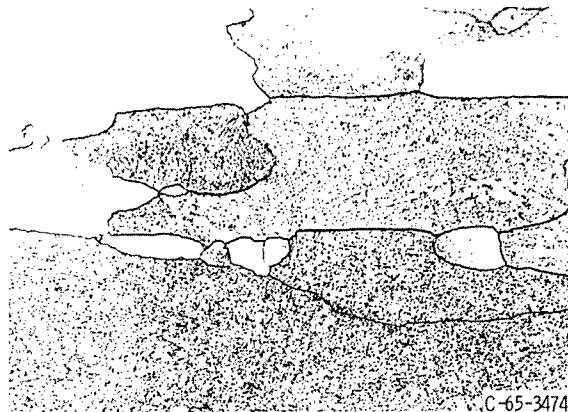
(b) Alloy C-2; tungsten - 0.33 atom percent carbon.



(c) Alloy CC-3; tungsten - 0.51 atom percent columbium - 0.29 atom percent carbon.



(d) Alloy TC-3; tungsten - 0.43 atom percent tantalum - 0.31 atom percent carbon.



(e) Alloy HC-3; tungsten - 0.20 atom percent hafnium - 0.26 atom percent carbon annealed at 4200° F for 4 hours. (Note lack of large carbides which were present in alloys in figs 15(b) to (d).) X250.

Figure 15. - Photomicrographs of carbide-strengthened alloys showing carbide distribution in (a) single-phase tungsten-columbium alloy, (b) tungsten-carbon alloy, (c) tungsten-columbium-carbon alloy, (d) tungsten-tantalum-carbon alloy, and (e) tungsten-hafnium-carbon alloy. All materials annealed at 3600° F for 1 hour. X250. (Reduced 25 percent in printing.)



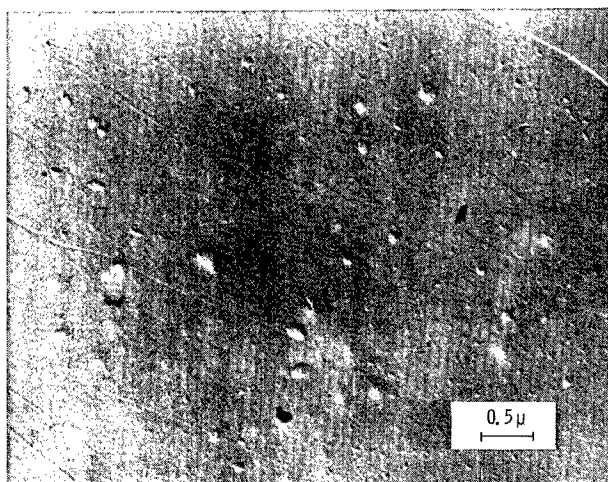
## Metallography of Carbide-

### Strengthened Alloys

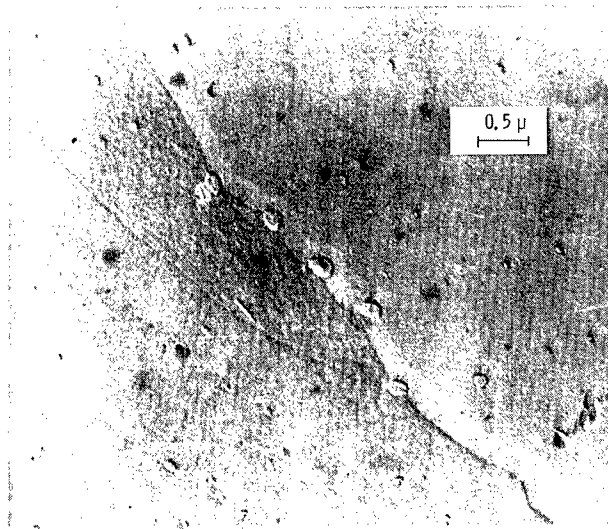
Metallographic studies were conducted on all the 3500° F tensile specimens of the W-Cb-C, W-C, W-Ta-C, and W-Hf-C alloys. The examinations were made on the undeformed button-heads of specimens that had been annealed for 1 hour at 3600° F prior to testing.

Figure 15(a) is typical of single-phase alloys. The specimen shows some etch pitting but is devoid of second-phase particles. The carbide structures in the W-C, W-Cb-C, and W-Ta-C alloys, shown in figures 15(b) to (d), represent similar carbon contents. A feature of these alloys was relatively coarse carbide size, with the particles tending to be aligned in the working direction. Figure 15(e) illustrates the microstructure of alloy HC-3, W - 0.20 atom percent Hf - 0.26 atom percent C after annealing for 4 hours at 4200° F and tensile testing at 3500° F. The grains are more elongated than those of the W-C, W-Cb-C, and W-Ta-C alloys in figures 15(b) to (d), and no carbide precipitates were observed at this magnification in spite of the fact that coarse carbides were observed in the as-melted condition (fig. 3(d), p. 8). These carbides were apparently dissolved into solid solution during processing.

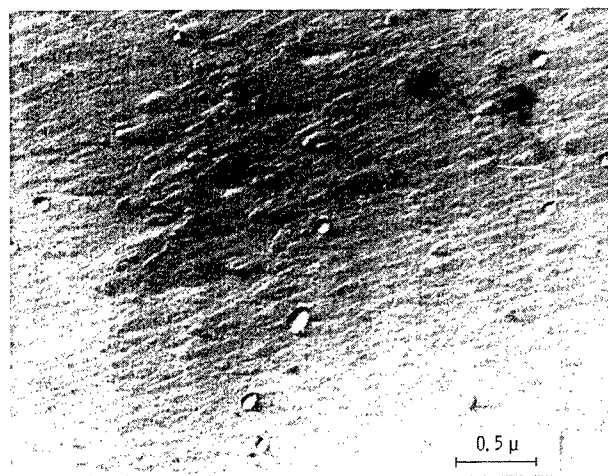
In view of the differences in the light microscopy results between the W-Hf-C alloys and the other carbon containing alloys, replica electron microscopy studies also were conducted on the W-Hf-C alloy. Sections of swaged rod from alloy HC-3 were annealed at 3600°, 3800°, 4000°, and 4200° F for 1 hour and furnace cooled. The percent recrystallized was estimated for each specimen. The W - 0.20



(a) Annealed 1 hour at 3600° F. X29 250.



(b) Annealed 1 hour at 4000° F. X29 250.



(c) Annealed 1 hour at 4200° F. X45 000.

C-65-3475

Figure 16. - Photomicrographs of carbide dispersion in tungsten - 0.20 atom percent hafnium - 0.26 atom percent carbon. (Reduced 55 percent in printing.)

atom percent Hf - 0.26 atom percent C alloy was only 50 percent recrystallized at 4200° F, while the unalloyed tungsten lot, W-1, attained this degree of recrystallization at 2300° F.

Electron microscopy results are shown in figure 16. A fine intragranular dispersion of carbide particles (presumably HfC or a complex W-Hf carbide) was observed with an occasional trace of coarser precipitation at the grain boundaries (fig. 16(b)). The carbide particle size ranged from approximately 0.05 to 0.2 micron, and no dependence of the carbide particle size on annealing temperature was observed, with the exception of a trace of additional grain-boundary precipitate in the materials annealed at 4200° F. As will be discussed in detail later, the fine carbide particle size in the W-Hf-C alloys probably accounts for the superior strengths of these alloys.

#### Low-Temperature Tensile Properties of Binary Tungsten-Carbon Alloys

The high-temperature tensile data on the binary W-C alloys were unusual in that little or no strengthening was achieved in spite of the presence of a carbide precipitate. The low-temperature tensile properties of these alloys were also studied near the ductile-brittle transition temperature to see if this behavior is consistent over the entire temperature range.

Figure 17 illustrates the low-temperature yield strength and percent elongation as a function of temperature for the binary W-C alloys and unalloyed tungsten. The strengths plotted for the W-C alloys are the lower yield strengths, as all the alloys yielded discontinuously. The data for unalloyed tungsten, W-1, includes both tensile and compressive proportional limits, as no yield points were observed.

The interesting results in figure 17 are that (1) the yield strengths of the W-C alloys increased continuously with carbon content in the temperature range 400° to 800° F, (2) the temperature dependence of the yield strength for the binary W-C alloys was greater than that for unalloyed tungsten, and (3) a measurable amount of ductility was observed at 400° F and the extrapolated ductility-temperature curves intersected the temperature axis at 150° to 200° F lower than that of unalloyed tungsten (the so-called "nil-ductility point", ref. 10). This effect on ductility is in sharp contrast to a previous investigation of the influence of carbon on the transition temperature of tungsten (ref. 11), where it was shown that carbon induced a sharp transition from ductile to brittle behavior and increased the nil-ductility temperature of tungsten.

#### DISCUSSION

##### Solid-Solution-Strengthened Alloys

The ultimate tensile strength of binary tungsten alloys at 2500° to 3500° F is plotted as a function of composition in figure 18. Included are data from references 1 and 12 in addition to the new results obtained for the

825

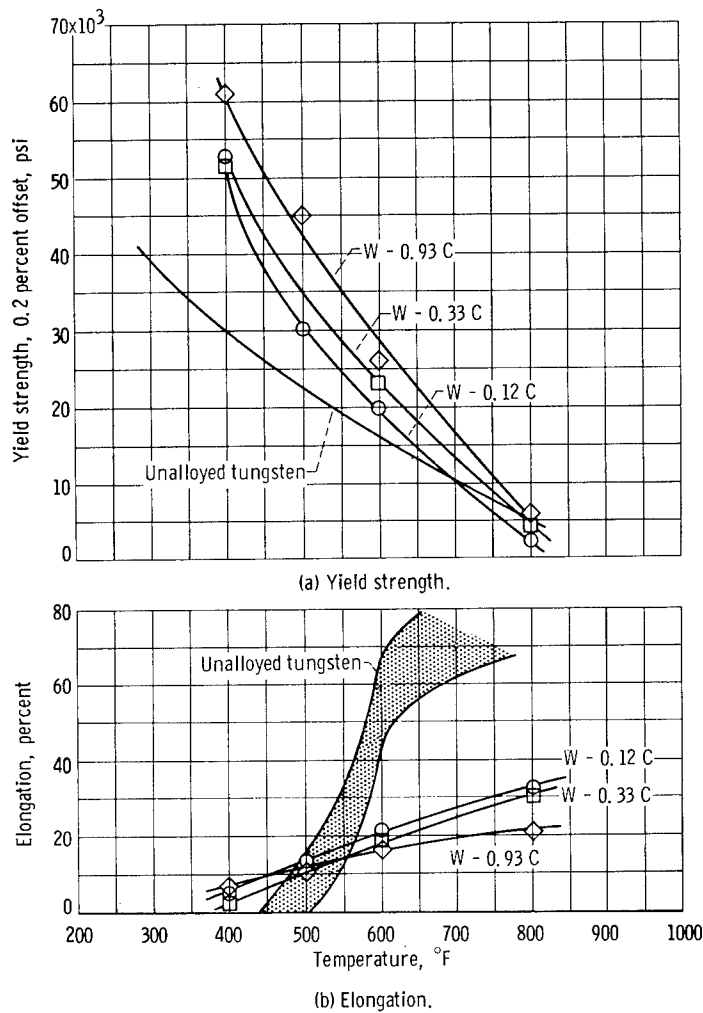


Figure 17. - Low-temperature tensile behavior of recrystallized tungsten-carbon alloys (compositions in atom percent).

W-Hf alloys in the present work. The curves drawn through the points represent fits on the data according to the relation

$$a_1 \sigma_u^2 + a_2 \sigma_u + a_3 = c$$

where  $\sigma_u$  is the ultimate tensile strength,  $c$  is the solute concentration in atom percent and  $a_1$ ,  $a_2$ , and  $a_3$  are constants. No great importance should be attached to the functional form of this equation as it was chosen only for convenience in calculating slopes of the curves and for interpolation. At 2500° to 3500° F, hafnium has the greatest strengthening effect in tungsten. Columbium, tantalum, and rhenium are progressively less effective. At 2500° F, the columbium and rhenium points fall on the same curve, and at 3500° F, the data for tantalum and columbium also scatter about one curve. The tantalum data are not shown at 3500° F for clarity; reference 1 may be consulted for details. Data at 4000° F were available only for hafnium and rhenium additions (not shown) and the same order of effectiveness prevailed.

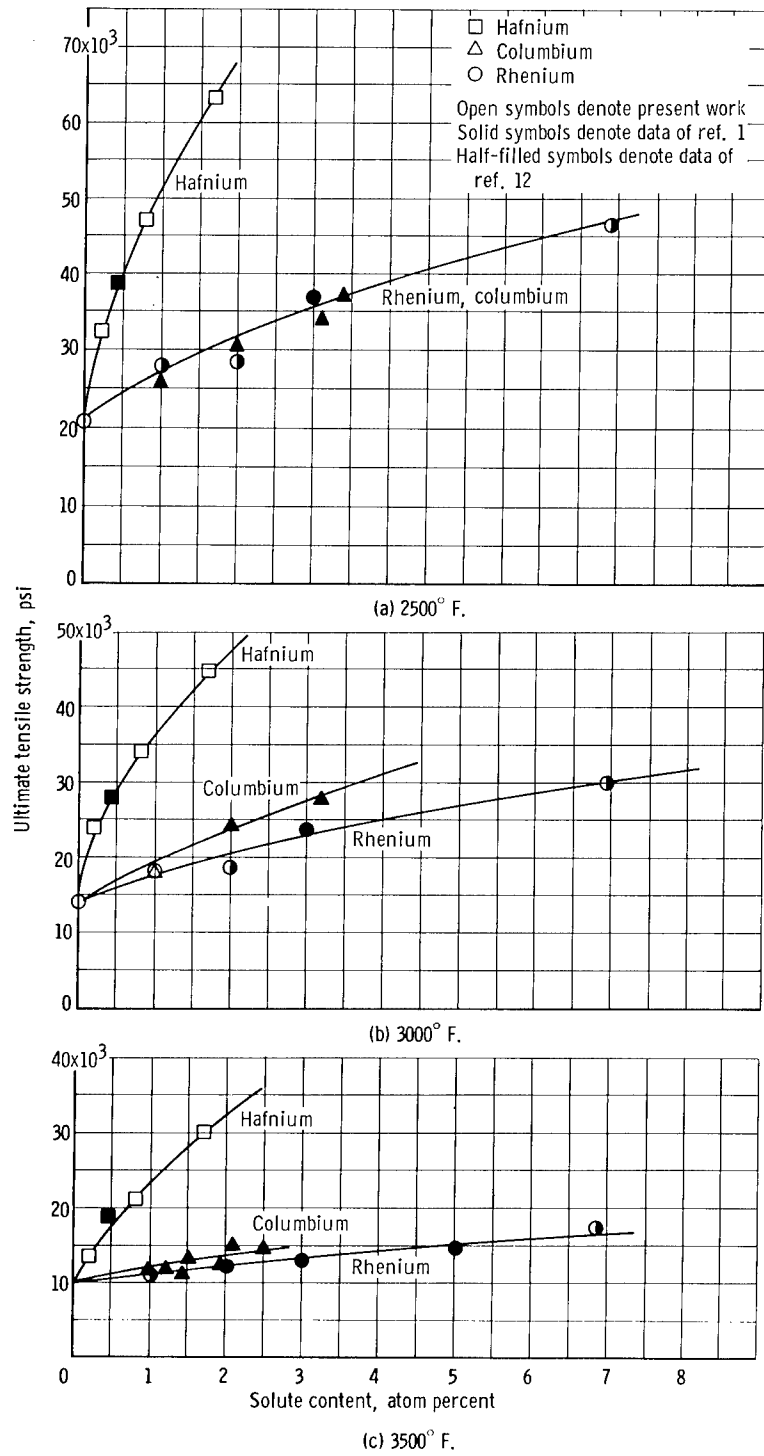


Figure 18. - Effect of alloying on strength of arc-melted tungsten at 2500° to 3500° F.

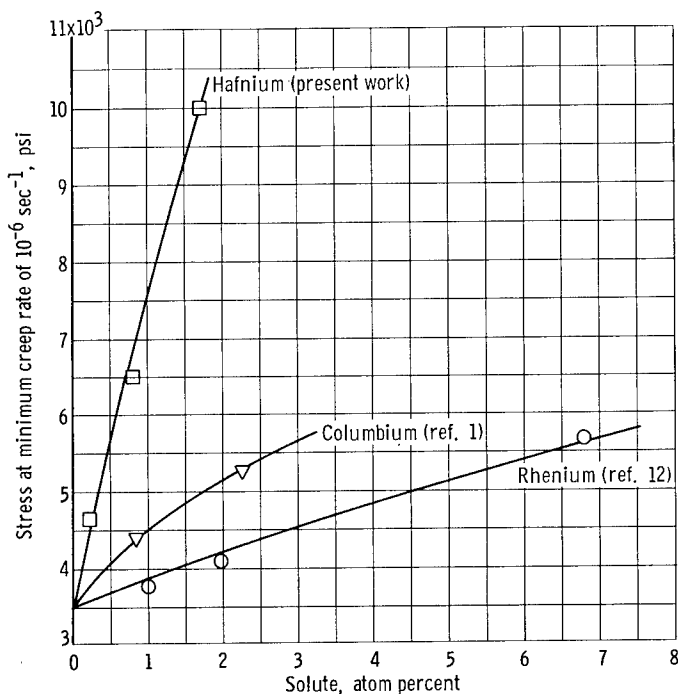


Figure 19. - Influence of alloying on 3500° F creep strength.

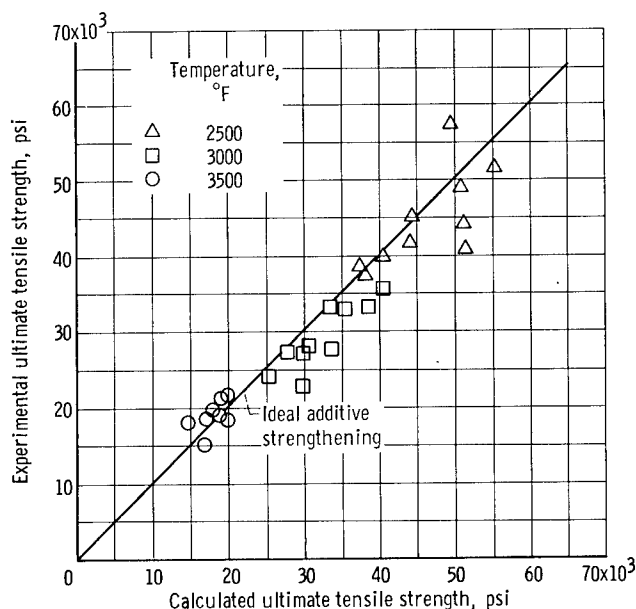


Figure 20. - Comparison of experimental tensile strengths with values calculated assuming additive strengthening effects. (Alloy systems include W-Ta-Re, W-Re-Hf, W-Ta-Hf, and W-Cb-Hf.)

The creep strengths for these binary systems at 3500° F are plotted against solute content in figure 19. The creep strengths are the stresses at a minimum creep rate of  $10^{-6}$  per second from the present work and references 1 and 12. The same order of effectiveness is apparent in the creep data as was observed in the tensile data. The curves in figure 19 are not fits of the functional relation used for the tensile data, but are approximated.

The tensile data for the binary alloys can also be utilized to predict the strength of the ternary alloys. It is a common conclusion that the solid-solution-alloying elements contribute the same increment of strength to a ternary as they do to a binary alloy (ref. 13). To test this for tungsten alloys, the increments of strengthening from the binary alloy data in figure 18 were calculated for each of the solutes in the W-Cb-Hf, W-Ta-Hf, W-Ta-Re, and W-Re-Hf ternary alloys. These increments were then added to the average strength for unalloyed tungsten at the temperature of interest. Figure 20 compares the calculated and experimental strengths for alloys annealed at 3600° F. The agreement with the assumption of additive strengthening is good especially when considering that no corrections were made for variations in grain size or interstitial contents among the alloys.

In order to understand the mechanisms by which the various solutes strengthen, the deformation mechanisms at elevated temperatures should be considered. Strain hardening in body-centered-cubic metals is thought to be related to the formation of jogs on screw dis-

locations by the interaction of dislocations on two intersecting slip planes (ref. 14). As the jogs move, they produce vacancies that act as a drag on the motion of the screw dislocations. However, the excess number of mechanically produced vacancies may promote climb of the edge segments of the dislocation networks. Such processes constitute "dynamic recovery" and as such reduce the rate of work hardening and consequently the elevated-temperature strength.

Alloying may increase the strength by decreasing either the jog or vacancy mobility. The motion of jogs may be impeded by solute atoms segregating to their stress field (ref. 15). Solute atoms and vacancies may also be strongly bound to one another (ref. 16). As a consequence, vacancies may tend to exchange places more often with solute than solvent atoms, which results in a lower self-diffusion rate since the vacancies are bound to the solute atoms and do not aid in solvent self-diffusion.

The strength of the binding between solute atoms and jogs or vacancies would be expected to depend on the difference in atom size between the solvent and solute (refs. 15 and 16). In reference 1, a qualitative correlation was made between the relative strengthening effect and this difference. In the present work, a more quantitative correlation was attempted by plotting the slopes of the strength-composition curves in figure 18 against the percent difference in atomic radius. Figure 21 illustrates this correlation. The log-log plot shown does indicate a definite atom size effect and provides support for the mechanisms outlined previously, although no estimation of the relative importance of solute-jog or solute-vacancy interactions can be deduced.

#### Strengthening of Carbon and Boron in Tungsten

Elevated-temperature tensile data have been obtained on both the W-C (see fig. 9, p. 17) and W-B systems (ref. 17). Carbon has been shown to exist as an interstitial in tungsten (ref. 18), while it has been proposed that boron may exist simultaneously as a substitutional and interstitial (ref. 19). A comparison of the strength data for both systems was made to examine whether or not the difference in the type of solid solution formed could have any influence on the elevated-temperature strength.

[Figure 22 shows the effect of both carbon and boron on the ultimate tensile strength of tungsten at 2500° and 3500° F. Carbon additions up to at least 0.3 atom percent decreased the strength, while in contrast, boron produced a rapid initial increase in strength followed by a leveling off at higher boron contents. The same trends were observed at 3000° and 4000° F.] It is believed that these differences between the W-C and W-B alloys reflect the previously mentioned differences in the type of solid solution formed. The initial strengthening by boron additions has been examined previously by the present authors who concluded that the magnitude of the initial slope of the strength-composition curve fit well with the concept of a simultaneous interstitial-substitutional solid solution with the balance tending toward substitutional (ref. 17). In contrast, carbon additions apparently weaken by promoting an increase in the self-diffusion rate of tungsten. This behavior has been previously noted for carbon additions to gamma iron (refs. 20 and 21). The increase in the self-diffusion rate has been suggested to result from the carbon

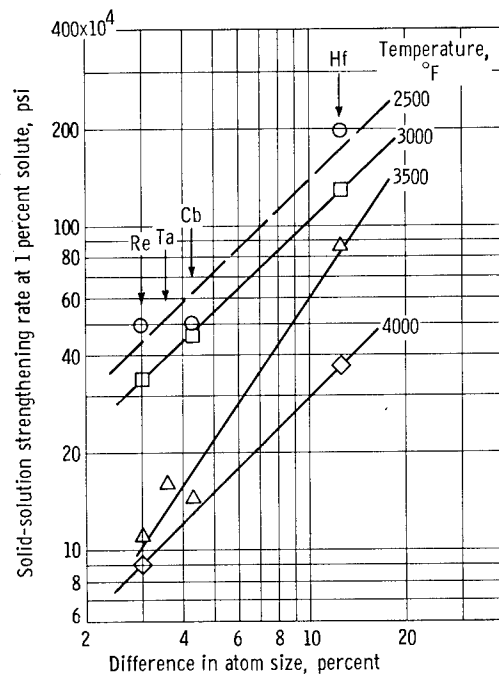


Figure 21. - Variation of solid-solution strengthening rate with difference in atom size between tungsten and solute.

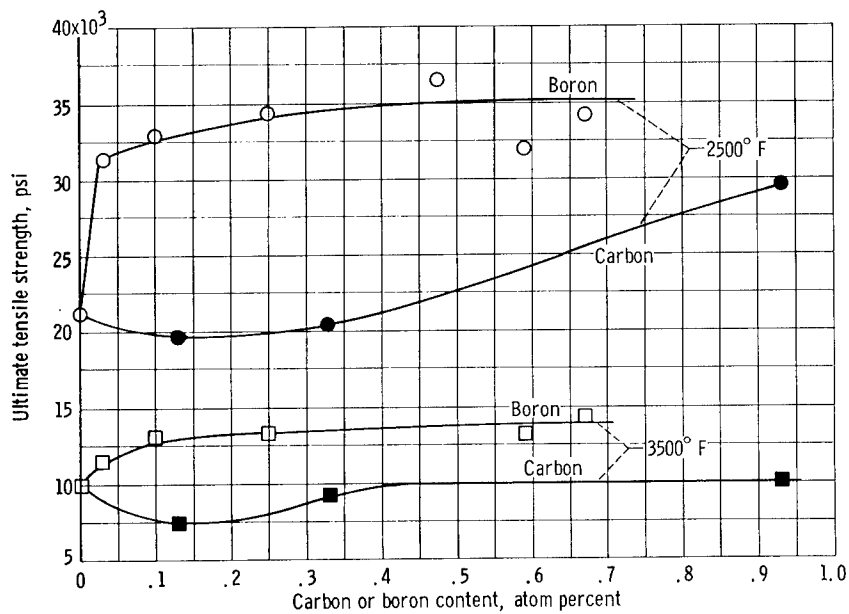


Figure 22. - Effects of carbon and boron on ultimate tensile strength of arc-melted tungsten at 2500° F and 3500° F (W-B data from ref. 7).

atoms increasing the vacancy mobility due to the lattice distortions associated with the interstitial solid solution (ref. 21).

### [Carbide-Strengthened Alloys]

The increase in strength conferred by carbon additions to W-Hf, W-Cb, W-Ta, and W-Ta-Re alloys will now be considered. As shown earlier, carbon additions to W-Hf alloys produced the greatest increases in both the strength of recrystallized alloys and in the retention of cold work at elevated temperatures.

[The relative strengthening effects of carbon on these alloys may be compared in the following manner. First, the strength of the alloy without the carbon addition is interpolated from the curves in figure 18. This value is

then subtracted from the strength of the alloy under consideration to give an increment in strength due to the carbon addition. Figure 23 is a plot of this strengthening increment as a function of carbon content for alloys tested at 3500° F. The data may be seen to fall into three groups. First, carbon additions to unalloyed tungsten result in an initial decrease in strength (which was discussed previously) followed by an increase in strength and a subsequent leveling off at higher carbon contents. In contrast, carbon additions to W-Hf alloys produced a rapid increase in strength, while the data for W-Cb, W-Ta, and W-Ta-Re alloys showed a less rapid increase. The data for the latter alloys showed a great deal of scatter and are represented by a broad band.]

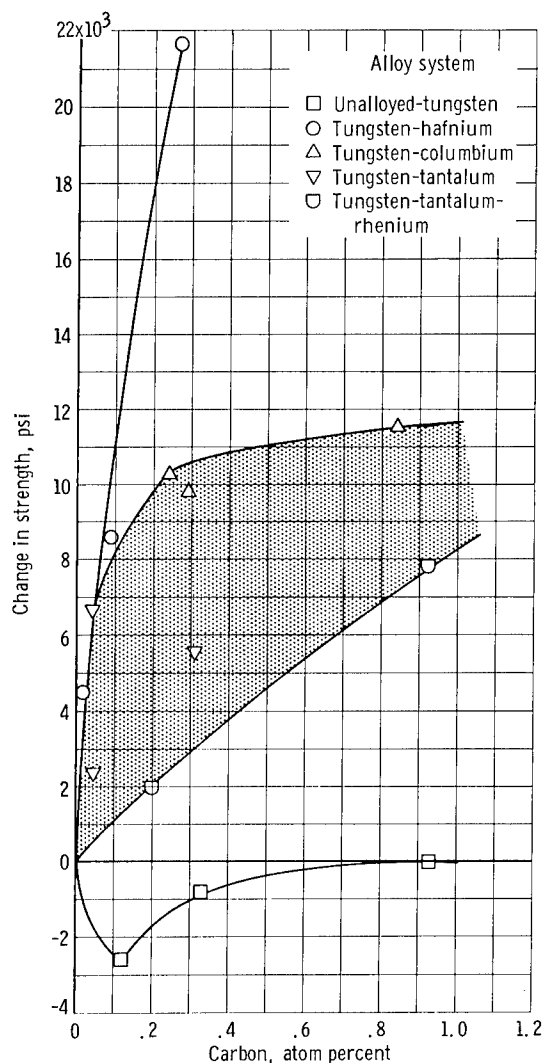


Figure 23. - Change in strength due to carbon additions to unalloyed tungsten and several tungsten alloy systems at 3500° F.

[These relative strengthening effects may be correlated qualitatively with the carbide particle size. The finest particle sizes were observed in the W-Hf-C alloys, as illustrated in figure 16(p. 23). In contrast, the carbides in the other systems were coarse and usually oriented in the swaging direction (fig. 15, p. 22). [The fine particles in the W-Hf-C alloys apparently are most effective in stabilizing the dislocation substructure formed during deformation. This is also evident in the high resistance to recrystallization exhibited by these alloys.]

[The coarse precipitates, however, contribute equally well to the strength at]



TABLE IX. - TENSILE STRENGTHS OF AS-SWAGED CARBIDE-STRENGTHENED ALLOYS AT 3000° AND 3500° F

Alloy, atom percent	Test temperature, °F	
	3000	3500
	As-swaged strength, psi	
W - 0.97 Ta - 2.62 Re - 0.92 C	85 300	25 700
W - 0.43 Ta - 0.31 C	84 100	16 600
W - 0.20 Hf - 0.26 C	88 200	62 500

[3000° F and lower, as the fine precipitates.] For example, the strengths of three carbide-strengthened alloys are compared in the swaged condition in table IX. The strengths at 3000° F for all the alloys are nearly equal while at 3500° F, the strengths vary from 16 600 to 62 500 pounds per square inch. This reflects largely the stability of the cold-worked structure. The first two alloys recrystallized during testing at 3500° F, while the W-Hf-C alloy retained its cold-worked structure.

[In creep, the fine particle sizes in the W-Hf-C alloys did not appear to produce as high strengths as found in some of the solid-solution-strengthened alloys.] For example, the creep strength of recrystallized HC-3, W - 0.20 atom percent Hf - 0.26 atom percent C was 8000 pounds per square inch at 3500° F, while alloys HF-3, W - 1.7 atom percent Hf, and TH-2, W - 1.56 atom percent Ta - 0.40 atom percent Hf had strengths of 10 000 and 8300 pounds per square inch, respectively, in spite of the W-Hf-C alloy having a higher tensile strength at this temperature.

Limited studies were conducted on the compositions of the carbides phase in these alloys. Particles extracted from alloy CC-3, W - 0.51 atom percent Cb - 0.29 atom percent C, were identified by X-ray diffraction as  $W_2C$ . The position of the lines was shifted slightly, indicating a slight expansion of the  $W_2C$  lattice possibly by dissolved columbium. Similar results were noted for a similar alloy in reference 1. Identification of the carbides in the other alloys could not be made because of experimental difficulties in extracting the particles from the matrix. The similar morphology of the carbides in the W-C, W-Cb-C, and W-Ta-C alloys, however, suggested that these were  $W_2C$  also. The carbides in the wrought W-Hf-C alloys had consistently finer particle sizes and were of a different morphology in the ingot than carbides in the alloys just described. It is believed that these carbides are HfC or a complex tungsten-hafnium carbide.

[The compositions of carbides formed in tungsten alloy systems can be estimated from consideration of free-energy data. Figure 24 shows the temperature dependence of the standard free energy of formation of some refractory carbides. The data for CbC, TaC, and HfC are calculated in reference 22, while the data for  $W_2C$  are calculated from references 23 and 24. It is seen from figure 24 that the stability of  $W_2C$  increases with increasing temperature, and precipitates formed in tungsten alloys containing carbon are a weak carbide.]

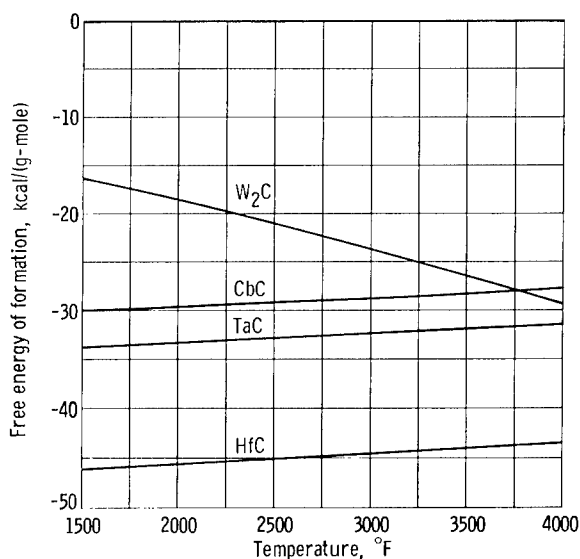


Figure 24. - Standard free energies of formation for selected refractory carbides.

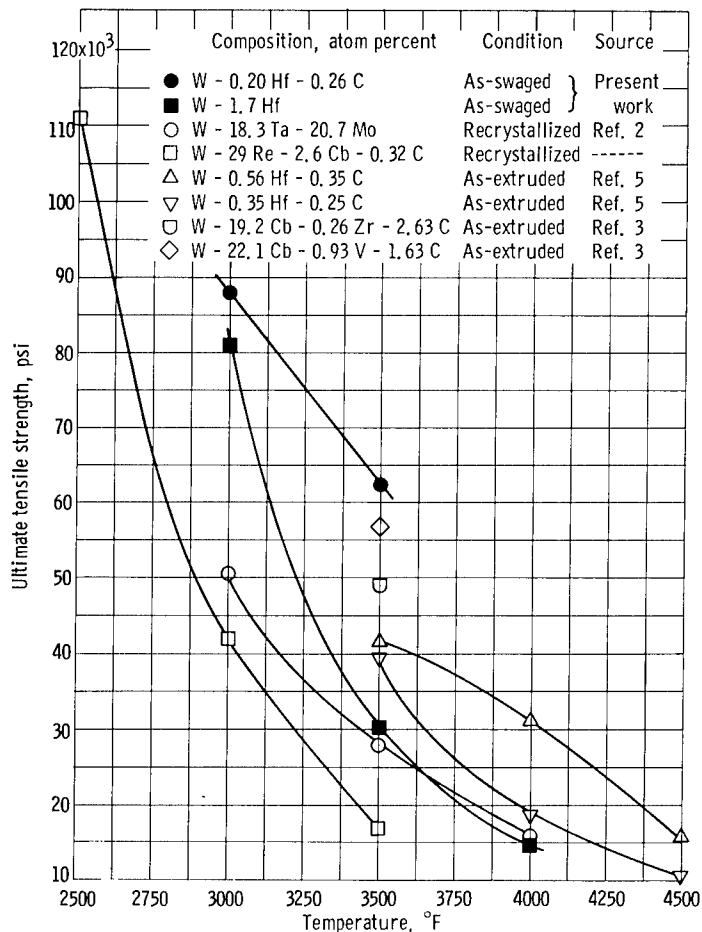


Figure 25. - Comparison of strongest alloys in present work with alloys from literature.

former, such as columbium or tantalum, should be predominantly W<sub>2</sub>C. In contrast, the estimated free energy of formation of HfC is larger than that of any of the other carbides. Thus, tungsten alloys containing hafnium and carbon should contain predominantly HfC.]

### Effects of Carbon on Low-Temperature Tensile Properties

The decreases produced in the "nil-ductility" temperature of tungsten by carbon additions in the range 0.12 to 0.93 atom percent were unexpected in light of previous investigations of the W-C system (ref. 11). In these previous alloys, the majority of the carbide precipitate was present at the grain boundaries, while in the present alloys, the major fraction of the carbide was stringered in the working direction and only a small amount was present in the grain boundaries. No explanation for the decreased transition temperature conferred by carbon additions is presently available.

### Practical Considerations

It is of interest to compare the properties of the most promising alloys investigated in this program and those in the literature. [Figure 25 shows the temperature dependence of the ultimate tensile strength for several arc-melted tungsten alloys.] It is interesting to note that some of the strongest tungsten alloys produced to date are in the W-Hf

and W-Hf-C systems. The data of reference 5 show that high strengths may be retained to temperatures as high as 4500° F with W-Hf-C alloys of the same type studied in the present work. In solid-solution-strengthened systems, the W - 1.7 atom percent Hf alloy from the present study was nearly identical in strength at 3500° to 4000° F to a W - 18.3-atom percent Ta - 20.7 atom percent Mo alloy from reference 2. The latter alloy had to be centrifugally cast to prevent ingot cracking, while the W - 1.7 atom percent Hf material from the present work could be successfully melted by more conventional techniques.

Thus it appears that future tungsten alloys for long-time use above 2500° F will very likely include alloys in the W-Hf and W-Hf-C systems. The possibility of employing dilute rhenium additions to these alloys to promote room temperature ductility is an additional factor that should be studied.]

### CONCLUSIONS

The following conclusions are drawn from this study on solution-strengthened and carbide-strengthened tungsten alloys consolidated by arc-melting:

1. The most effective solid-solution strengthener in tungsten of those evaluated in this study is hafnium. Rhenium is the least effective. The same order holds in creep as in tension.
2. The relative solid-solution-strengthening effects could be correlated with the difference in atom size between tungsten and the solute atom.
3. The strengths of ternary solid solution alloys could be represented as the sum of the individual effects found in the binary alloys at 2500° to 3500° F. Tungsten-tantalum-rhenium alloys showed greatly enhanced resistance to recrystallization at 3500° F.
4. Carbon additions to tungsten-columbium, tungsten-tantalum, tungsten-tantalum-rhenium, and tungsten-hafnium alloys produced various degrees of strengthening. The greatest strengthening was found in the tungsten-hafnium-carbon system. The strongest alloy, tungsten - 0.20 atom percent hafnium - 0.26 atom percent carbon, had strengths of 88 200 and 62 500 pounds per square inch in the worked condition at 3000° and 3500° F, respectively. The differences in strength between the various carbide-strengthened alloys were related to differences in carbide particle size. The particle size in the tungsten-hafnium-carbon alloys was the finest, on the order of 0.05 to 0.20 micron.
5. Carbon additions to unalloyed tungsten at 2500° to 4000° F produced a minimum in the strength - carbon-content curve. This behavior may be caused by an increase in the self-diffusion rate of tungsten caused by carbon. The nil-ductility transition temperature of tungsten was decreased by carbon additions in the range 0.12 to 0.93 atom percent.] → P34

Lewis Research Center,  
National Aeronautics and Space Administration,  
Cleveland, Ohio, November 3, 1965.

## REFERENCES

- [1. Raffo, Peter L.; Klopp, William D.; and Witzke, Walter R.: Mechanical Properties of Arc-Melted and Electron-Beam-Melted Tungsten-Base Alloys. NASA TN D-2561, 1965.]
2. Stefan, Lawrence J.; Lake, Frank N.; and Cook, Charles R.: Research on Refractory Alloys of Tungsten, Tantalum, Molybdenum and Columbium. Rept. No. ML-TDR-64-271, Thompson Ramo Wooldridge, Inc., Sept. 1964.
3. Westgren, R. C.; and Thompson, V. R.: Dispersion-Strengthened Refractory Alloys. Trans. AIME., vol. 230, no. 4, June 1964, pp. 931-934.
4. King, G. W.; and Sell, H. G.: The Effect of Thorium on the Elevated-Temperature Tensile Properties of Recrystallized High-Purity Tungsten. Trans. AIME, vol. 233, no. 6, June 1965, pp. 1104-1113.
5. Semchyshen, M.; and Kalns, Eric: Tungsten-Base Alloy Development. Paper Presented at AIME Conf. on Phys. Metallurgy of Refractory Metals, French Lick (Ind.), Oct. 3-5, 1965.
6. Quatinetz, Max.; Weeton, J. W.; and Herbell, T. P.: Studies of Tungsten Composites Containing Fibered or Reacted Additives. NASA TN D-2757, 1965.
- [7. Foyle, Fred A.: Arc-Melted Tungsten and Tungsten Alloys. High Temperature Materials, Vol. 18, Pt. II, G. M. Ault, W. F. Barclay and H. P. Munger, eds., Intersci. Pub. Inc., 1963, pp. 109-124.]
8. Noesen, Stanley J.: The Removal of Gaseous Impurities by Vacuum Arc Melting. 1957 Vacuum Symposium Trans., Pergamon Press, 1958, pp. 150-156.
9. Klopp, William D.; and Raffo, Peter L.: Effects of Purity and Structure on Recrystallization, Grain Growth, Ductility, Tensile, and Creep Properties of Arc-Melted Tungsten. NASA TN D-2503, 1964.
10. Seigle, L. L.; and Dickinson, C. D.: Effect of Mechanical and Structural Variables on the Ductile-Brittle Transition in Refractory Metals. Refractory Metals and Alloys, Vol. 17, Pt. II, M. Semchyshen and I. Perlmutter, eds., Intersci. Pub. Inc., 1963, pp. 65-116.
11. Stephens, Joseph R.: Effects of Interstitial Impurities on the Low-Temperature Tensile Properties of Tungsten. NASA TN D-2287, 1964.
- [12. Klopp, W. D.; Witzke, W. R.; and Raffo, P. L.: Properties of Dilute Tungsten-Rhenium Alloys. Paper Presented at AIME Conf. on Phys. Metallurgy of Refractory Metals, French Lick (Ind.), Oct. 3-5, 1965.]
- [13. Parker, E. R.; and Hazlett, T. H.: Principles of Solution Hardening. Relation of Properties to Microstructure, ASM, 1954, pp. 30-70.]

-p35

14. Gregory, Donald P.; Rowe, George H.; and Stroh, Alan N.: Work Hardening Mechanisms in Body-Centered Cubic Metals. Rept. No. ASD-TDR 62-354, Pratt & Whitney Aircraft, Sept. 1962.
15. McLean, D.: Mechanical Properties of Metals. John Wiley & Sons, Inc., 1962.
16. Eikum, A.; and Thomas, G.: Effect of Solute Atoms Upon Vacancy Climb of Prismatic Dislocations in Al-5 % Mg Alloy. Phys Soc. Japan J., vol. 18, suppl. III, 1963, pp. 98-104.
17. Raffo, Peter L.; and Klopp, William D.: Influence of Boron Additions on Physical and Mechanical Properties of Arc-Melted Tungsten and Tungsten - 1 percent Tantalum Alloy. NASA TN D-3247, 1966.
18. Goldschmidt, H. J.; and Brand, J. A.: Investigation Into the Tungsten-Rich Regions of the Binary Systems Tungsten-Carbon, Tungsten-Boron and Tungsten-Beryllium. Rept. No. ASD-TDR-62-25, pt. 1, Birmingham Small Arms Res. Centre, Mar. 1962.
19. Goldschmidt, H. J.; Catherall, E. A.; Ham, W. M.; and Oliver, D. A.: Investigation Into the Tungsten-Rich Regions of the Binary Systems Tungsten-Carbon, Tungsten-Boron and Tungsten-Beryllium. Rept. No. ASD-TDR-62-25, pt. II, Birmingham Small Arms Res. Centre, July 1963.
20. Sherby, O. D.: Factors Affecting the High Temperature Strength of Polycrystalline Solids. Acta Met., vol. 10, no. 2, Feb. 1962, pp. 135-147.
21. Mead, H. W.; and Birchenall, C. E.: Self-Diffusion of Iron In Austenite. Trans. AIME, vol. 206, Oct. 1956, pp. 1336-1339.
22. Kaufman, L.; and Sarney, A.: Thermodynamic Properties of Transition Metal Monocarbides. Nuclear Metallurgy. Vol. X - Compounds of Interest in Nuclear Reactor Technology. AIME, 1964, pp. 267-279.
23. Mah, Alla D.: Heats of Combustion and Formation of Carbides of Tungsten and Molybdenum. Rept. No. BM-RI-6337, Bur. Mines, 1963.
24. Kelley, K. K.: Contributions to the Data on Theoretical Metallurgy. XIII. High-Temperature Heat-Content, Heat-Capacity, and Entropy Data for the Elements and Inorganic Compounds. Bull. No. 584, Bur. Mines, 1960.

end

*"The aeronautical and space activities of the United States shall be conducted so as to contribute . . . to the expansion of human knowledge of phenomena in the atmosphere and space. The Administration shall provide for the widest practicable and appropriate dissemination of information concerning its activities and the results thereof."*

—NATIONAL AERONAUTICS AND SPACE ACT OF 1958

## NASA SCIENTIFIC AND TECHNICAL PUBLICATIONS

**TECHNICAL REPORTS:** Scientific and technical information considered important, complete, and a lasting contribution to existing knowledge.

**TECHNICAL NOTES:** Information less broad in scope but nevertheless of importance as a contribution to existing knowledge.

**TECHNICAL MEMORANDUMS:** Information receiving limited distribution because of preliminary data, security classification, or other reasons.

**CONTRACTOR REPORTS:** Technical information generated in connection with a NASA contract or grant and released under NASA auspices.

**TECHNICAL TRANSLATIONS:** Information published in a foreign language considered to merit NASA distribution in English.

**TECHNICAL REPRINTS:** Information derived from NASA activities and initially published in the form of journal articles.

**SPECIAL PUBLICATIONS:** Information derived from or of value to NASA activities but not necessarily reporting the results of individual NASA-programmed scientific efforts. Publications include conference proceedings, monographs, data compilations, handbooks, sourcebooks, and special bibliographies.

*Details on the availability of these publications may be obtained from:*

SCIENTIFIC AND TECHNICAL INFORMATION DIVISION  
NATIONAL AERONAUTICS AND SPACE ADMINISTRATION  
Washington, D.C. 20546